Thermal hydraulic feasibility of upgrading the JEEP II heavy water research reactor from 2 to 5 MW

Erik Henriksen

Norwegian University of Life Sciences
Department of Mathematical Sciences and Technology
Master Thesis 30 credits 2013

This page is left blank intentionally

THERMAL HYDRAULIC FEASIBILITY OF UPGRADING THE JEEP II HEAVY WATER RESEARCH REACTOR FROM 2 TO 5 MW

Erik Henriksen

17. January 2013

PREFACE

This master thesis marks the end of my studies, a five year master programme in Environmental Physics and Renewable Energy at the University for Life Sciences in Ås. Being able to write a thesis revolving around general physics was of importance for me, so when the topic of thermal hydraulics was presented for me by Ole Reistad and Sverre Hval at IFE I immediately decided to go through with it. Writing the thesis at IFE was assuring; the skilled engineers and physicist could answer any questions I had.

I would like to thank my advisor at IFE, Steven Mullet, for much help. Thanks to you, Matlab is now no longer so scary, and physics is just that more fun. Big thanks to Arne Auen Grimenes, my advisor at UMB. Thank you for helping me with my thesis and giving council and support throughout the semester. I would also like to thank my "secondary advisor", Ole Reistad at IFE. Thanks for great conversations, help with my thesis and the races from Lillestrøm to Oslo with your electric car.

I am very happy for the great years at Ås. My fellow classmates have supported me along the way, giving me confidence that the future is green and in good hands. Ås also has so many great teachers that have given me inspiration to continue my studies and become more interested in physics. Thank you all for the good times.

A special thanks to my family, keeping me motivated through the writing.

Table of Contents

SUMMARY

This thesis examines the thermal hydraulic feasibility of a power upgrade of the JEEP II research reactor at Institutt for Energiteknikk (IFE). The 2 MWth reactor is modelled in Matlab, a programming language and numerical computing environment. The Matlab script will execute calculations for a fuel pin within a fuel element and the surrounding heavy water, and find heat transfer characteristics, heat fluxes and temperatures. A conservative approach is taken, resulting in maximum values for temperatures and heat fluxes. Tabulated and empirical values from the reactor operation are used to verify the validity of the model. The model of the 2 MWth reactor is then extrapolated to a power of 5 MWth. Mitigating measures to reduce the associated high temperatures from the power extrapolation are taken in the Matlab script. The upgrade is deemed feasible when the 5 MWth fuel pin temperatures and heat flux are equal to or lower than the 2 MWth temperatures and heat flux.

SAMMENDRAG

Denne masteroppgaven undersøker hva slags innvirkninger en effektoppgradering av forskningsreaktoren JEEP II vil ha. Reaktoren, som har en termisk effekt på 2 MW, er modellert i Matlab; et programmeringsspråk som opererer i matriser. Matlab-skriptet vil utføre beregninger for en brenselspinne i et brenselselement og tungtvannet som sirkulerer i brenselselementet. Matlab-skriptet utformes for å regne ut brenselspinnens forskjellige temperaturer og varmefluks. Beregningene utføres med en konservativ fremgangsmåte, noe som resulterer i maksimumsverdier av temperaturer og varmefluks. Tabulerte og empiriske verdier fra reaktorens operasjon er brukt for å verifisere gyldigheten til modelleringen, og modellen ekstrapoleres til en ny termisk effekt; 5 MW. Tiltak gjennomføres for å redusere de tilhørende høye temperaturene fra ekstrapoleringen. Oppgraderingen er vurdert som gjennomførbar når brenselspinnetemperaturene og varmefluksen ved 5 MW er lik eller lavere enn brenselspinnetemperaturene og varmefluksen ved 2 MW.

1. Introduction

Research question

The topic for this thesis is the feasibility of a power upgrade from 2 to 5 MW of the JEEP II heavy water research reactor. This would lead to improved research facilities, however, there is a need maintain fundamental properties, such as heat flux and fuel and cladding temperatures, of the reactor at the same level as for the present reactor due to safety reasons.

From this follows the research question of the thesis: can the temperatures and the heat flux in the fuel pins of the reactor be kept at 2 MW levels after a power upgrade from 2 to 5 MW?

As a nuclear reactor is a complicated technological system, such a feasibility study calls for careful consideration of limitations in the thesis, previous and similar efforts in this regard, the methodological approach and assessment of the results. This constitutes the main parts of this thesis as presented below.

Thesis approach and structure

The methodological approach is to model the 2 MW reactor in Matlab. This model is then verified on the basis of empirical values from operation of the reactor. The temperatures and heat transfer properties of the fuel and heavy water are identified through calculations of convective and conductive properties.

The results from modelling the present 2 MW reactor are then extrapolated to 5 MW, yielding higher temperatures in the fuel pin and the heavy water. The resulting fuel cladding temperatures in the 5 MW model were 100˚C above the results from the 2 MW model. This increases the possibility for a departure from nucleate boiling at the fuel pin cladding surface. The resulting fuel centre line temperatures in the 5 MW model were 1 800 ˚C higher than the results

from the 2 MW model, and above the melting point of uranium dioxide. Mitigating measures include changes in the geometry of the core and the fuel elements, and changes in the volumetric flow rate. This reduced the overall fuel pin temperatures. The mitigating measures were then combined, aiming to reduce the temperatures further down to the levels associated with operating the reactor on 2 MW.

Chapter 2 described the status today for commercial and research reactors. Chapter 3 contains the theory necessary to model the heat transfer in the fuel pins and the heavy water in the reactor. This includes basic heat and thermal hydraulic equations for conductive and convective heat transfer in different geometries and aggregates. This chapter also addresses nuclear physics theory, introducing, describing and applying the fundamental concepts. This is included as the topic is based on a nuclear research reactor.

Chapter 4 presents the method and the empirical material for the thesis. This includes the schematics of the core and the primary coolant circuit system, and the flow scheme of the heavy water in the primary coolant circuit. The empirical values from the operation of the JEEP II are listed here. The chapter then describes the modelling of the 2 MW reactor, beginning with the assumptions used as a basis for the model, leading into how the heat transfer from the fuel pin to the heavy water was found through different flow correlations. The heat equations for finding the temperatures from the cladding of the fuel pin to the fuel centre line are then presented, including considerations on sensitivity and data uncertainty analysis. Then the extrapolation to 5 MW is shortly addressed.

Chapter 5 contains the results from the application of the 2 MW and 5 MW model. Firstly, the fuel pin temperatures and the heat flux are presented as a distribution peaking at the midpoint of the fuel pin. The different Nusselt correlations for the flow regime and the following heat transfer coefficients are also included here. The mitigating measures are then introduced, starting off with the considering the options for geometrical changes. Then the effects of increasing the volumetric flow rate are described. Lastly, the combined effect of increased volumetric flow rate with constant heavy water velocity

through a fuel element and the two most promising geometrical measures is considered qualitatively.

Chapter 6 discusses the 2 MW and 5 MW model. The discussion considers safety, the feasibility of the 2 MW model, and the nominal and mitigated 5 MW model and the various mitigating measures. A short error analysis is included in chapter 6. Chapter 7 contains the conclusion of this thesis.

LIMITATIONS

This thesis covers mainly the potential and constraints regarding thermal hydraulics associated with the upgrade to 5 MW, this means that the nuclear physics part of the reactor of fission within the fuel pellets and the associated neutronics is addressed only when necessary. The focus of this thesis is the heat flux and the temperatures in the fuel pins, which is why the modelling script only calculates the heat flux and the temperatures for the fuel pins and the surrounding bulk of heavy water. The circuit systems of the primary, secondary and tertiary coolant loops are not considered, i.e. the script calculates the properties only for the fuel pins and the surrounding heavy water.

PREVIOUS WORK

A literature study was carried out to find previous work done on research reactors, where the alteration or upgrading of research reactors were of special interest. Previous reports on an upgrade of the JEEP II had been written at IFE, mainly focusing on a higher neutron flux for better research conditions and the possibility of conducting more in depth research on materials [1]. The proposed upgrading of the power was discarded due to the need for major changes to be done on the core and the reactor, and because the work load, down time and risks were deemed too large [2]. A report written by H. Sækkeseter describes an accident situation where the JEEP II core melted due

to loss of coolant [3]. A detailed look on the melting point of the fuel pin cladding for different geometries is included here. A. Lundbergs report on burnout calculations of the JEEP II gives a conservative burnout flux for 2 MW [4]. The article written by H. E. Andås and Th. Ustaheim describes the consequences of a full stop of the heavy water circulation in the core [5]. Here the temperatures of the fuel pin and coolant after a reactor scram are listed. A report written by T. Hernes contains thermal hydraulic calculations on the fuel pins and the heavy water, and specifics of the core, inter alia the fuel elements, are listed here [6]. S. Mullet wrote an article that investigated if natural circulation of heavy water could cool the core [7]. This article contains specifics about the core, and has an appendix with useful calculations.

A report on the High Flux Reactor in Petten, The Netherlands, has been of particular interest, as it describes how the power upgrading of the Petten reactor from its original power of 20 MW via 30 MW to 45 MW was done [8]. The upgrade improved the research capabilities of the reactor, and the cooling systems with heat exchangers and pumps were replaced. A paper from Cairo University included a thermal hydraulic modelling of an accident situation in a materials testing reactor [9]. This paper gave valuable insight in thermal hydraulic calculations and reactor modelling.

The JEEP II

The JEEP II research reactor is located at Kjeller, Lillestrøm, and is operated by IFE. The JEEP II went critical for the first time in 1966, as an upgrade from the JEEP I reactor [10]. It is a 2 MW low flux reactor with heavy water as the coolant and moderator. Since this is a research reactor that does not produce electricity, the power level given above describes thermal energy production, and this will be the default in this assignment. This means that all the listed powers here are thermal, when not mentioned otherwise. The upgrade was undertaken to make activities such as neutron physics and isotope production more accessible. The work undertaken at JEEP II consists of transmutation doping of silicon for the solar cell industry and research, material research with neutron optics and production of radio nuclear medicine [11].

The JEEP II has a low neutron flux compared to other research reactors, an incentive for upgrading the power. Over the years, the physicists at the JEEP II have become more creative in utilizing the neutron flux coming from the 2 MW power when conducting research and work [2]. There is a consensus at IFE wanting a higher neutron flux to be able to conduct the conventional basis research in a better and faster way, and to explore new experimental methods in material research [11]. There is also a wish to improve the irradiation facilities, primarily associated with the research and work IFE completes for the semiconductor industry.

The term "neutron drought" was coined in the 1990's in Europe. The European Neutron Scattering Association concluded in a report from 1996 that there was a demand of 78 % more beam time at High Flux Reactors to be able to execute the current research programmes efficiently [12]. A report from OECD from 1994 on the availability of neutrons predicted a dramatic failure in the amount of neutron sources and the measuring capacity, which is shown in Figure 1. The failure in the amount of neutron sources is also an incentive for upgrading the JEEP II.

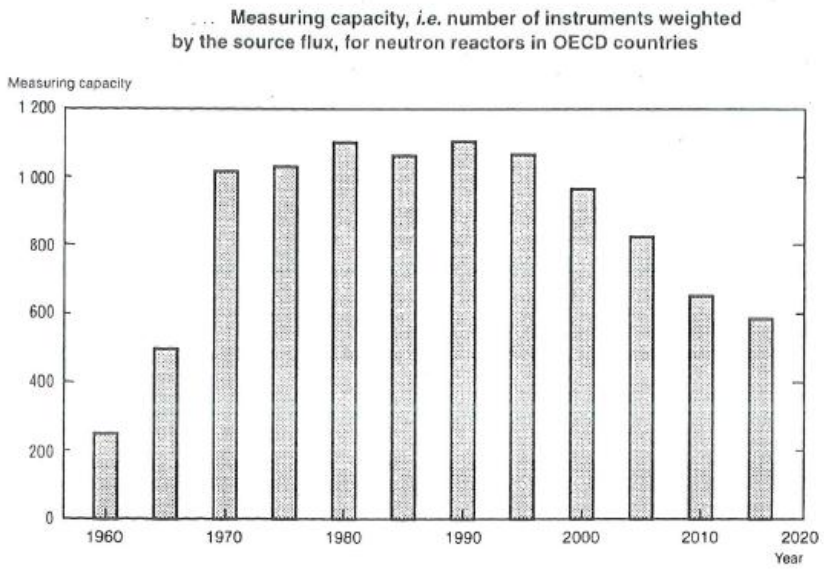

Figure 1. *Changes in the measuring capacity for neutron scattering in OECD countries from 1960 to 2020* [11].

2. BACKGROUND

NUCLEAR POWER TODAY

In the world today there are over 430 commercial nuclear power reactors operating in 31 countries [13]. The total capacity of all these reactors are 372 000 MWe. The thermal efficiency of a general commercial nuclear reactor is around 33-37 % [14]. Commercial reactors operate as electricity producers, converting energy from fission reactions in the core of the reactors. In 2012, commercial nuclear power reactors provided about 13.5 % of the total electricity production of the world [13]. The most common models of nuclear reactors are *boiling water reactors* (BWR) and *pressurized water reactors* (PWR), where Figure 2 shows the schematics of a PWR.

The future of nuclear energy is uncertain because of the concern for nuclear safety coming from large nuclear accidents as Fukushima and Chernobyl, the large capital investments involved in nuclear power plant construction, the proliferation risks and waste concerns [15].

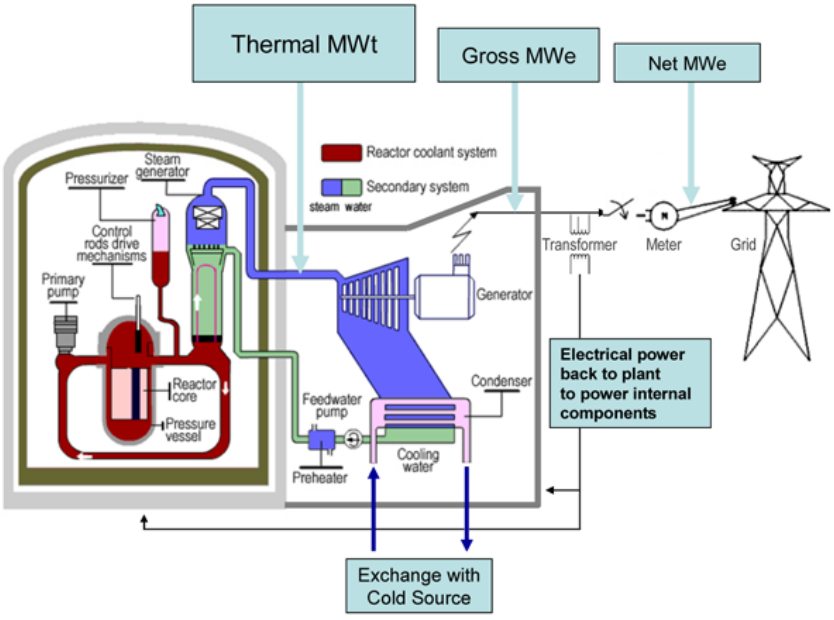

Figure 2. Schematics of a PWR [16].

RESEARCH REACTORS

There are today a total of about 240 research reactors in operation in 56 countries [13]. These reactors are used for research within different fields, such as materials testing, the production of radioisotopes for medicine and industry, neutron optics and fuel testing [17]. The most common design is a pool type reactor where the core is a bundle of fuel elements submerged in water. Research reactors in Europe are amongst other the Petten reactor, a 45 MW high flux reactor, and the FRM II in Munich, a 20 MW high flux reactor. Figure 3 shows an extract of the Petten reactor building. Research reactors operate at much lower temperatures than commercial reactors, and they need less fuel. The enrichment grade is usually higher in research reactors since a high flux is paramount to conduct research. The enrichment grade is typically around 20 % U-235, which means that the fuel contains 20 % U-235, and 80 % U-238 [17].

Figure 3. Cross section of the Petten High Flux Research Reactor in The Netherlands [18].

3. THEORY

NUCLEAR PHYSICS

NUCLEAR MASS AND ENERGY

The nuclear mass is ca. 1 % smaller than the mass of its constituent nucleons; its individual protons and neutrons [19]. This difference is given as the mass defect, or in other words the energy required splitting the nucleons forming the nucleus. This energy is referred to as the binding energy, and helps to explain how stable a nucleus is and how much energy that is released in a nuclear reaction [19]. Mass and energy has an equivalence relationship which is presented in (1)

$$E = mc^2 \qquad (1)$$

where E is the energy, m is the mass defect and c is the speed of light.

The binding energy directly affects the mass of an atom [20]. When 1 g of matter is completely converted energy equal to 20 000 tons of TNT is released. The scale of mass used in atomic calculations is called the atomic mass unit, u, where 1 u is equivalent to 931.5 MeV/c^2. The mass defect of a nuclear reaction is usually small, but the associated energy is large due to the multiplication of the square of the speed of light.

Nuclei are bound together by the nuclear force [20]. The nuclear force must compensate for the repulsive Coulomb force between protons; therefore there is an increasing amount of neutrons with respect to protons the larger the nucleus gets. The nuclear binding per nucleon energy thus increases, as shown in Figure 4. The stronger Coulomb force makes the binding energy per nucleon to fall from its peak point of 8.6 MeV.

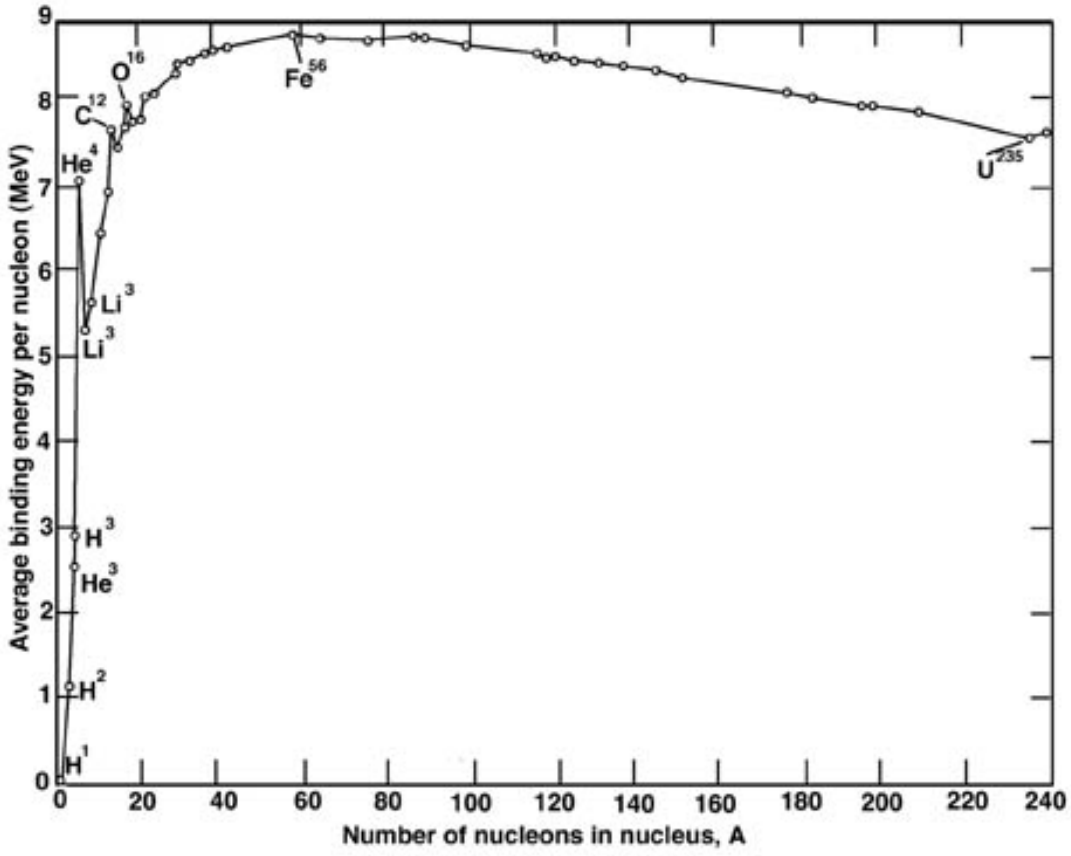

Figure 4. Average binding energy BE per nucleon A [21].

FISSION

The nuclear reaction of fission occurs when a nuclei absorbs a neutron and subsequently splits into smaller parts [20]. U-235 is selected as an example due to its widespread use in commercial and research reactors. In a fission reaction, a neutron combines with the fissile nucleus of U-235 and the excited U-235 atom subsequently fissions. A probable outcome of a fission event for U-235 atom is illustrated in Figure 5.

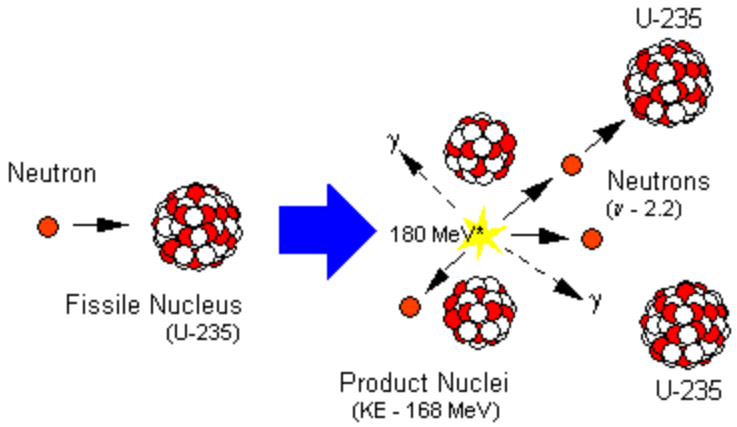

Figure 5. Fission reaction of U-235 and the possible outcome [22].

The outcome of fission is a probabilistic process. The yield of fission depends on the fissioned nucleus and the energy of the incident neutron [23]. The possible product nuclei all have associated probabilities of occurring, referred to as the fission chain yield. The total number of neutrons following the fission also varies, with an average number of 2.43 for the fission of U-235 [23]. A possible result for the fission of U-235, as shown in Figure 5 is an energy yield of 180 MeV, released energy in the form of gamma radiation, two product nuclei and three fast neutrons. The neutrons from the fission can either continue the fission reaction with other fissile targets, or collide with other materials thus reducing their energy.

Controlled fission

Fission is controlled within reactors to be able to extract the kinetic energy coming from the fission reactions. Commercial reactors use fuel that has typically been enriched to 3-5 % prior to loading into the reactor [24]. To increase the possibility of absorption of a neutron with a fissile target, the neutron energy must be moderated from higher to lower energy. Neutrons with energy in the MeV range are called fast neutrons and neutrons with energy in the eV range are called thermal neutrons [23]. Every type of interaction has an associated incident neutron nuclear cross section that represents the probability that a specific type of nuclear reaction will occur

when different isotopes are struck by a neutron [23]. Many different types of neutron incident reactions are possible, each with an associated cross section. The nuclear cross section can generally be grouped into three parts; absorption, scattering and fission, and has the unit barns, which is 10^{-24} cm^2. Figure 6 shows the fission cross section of U-235.

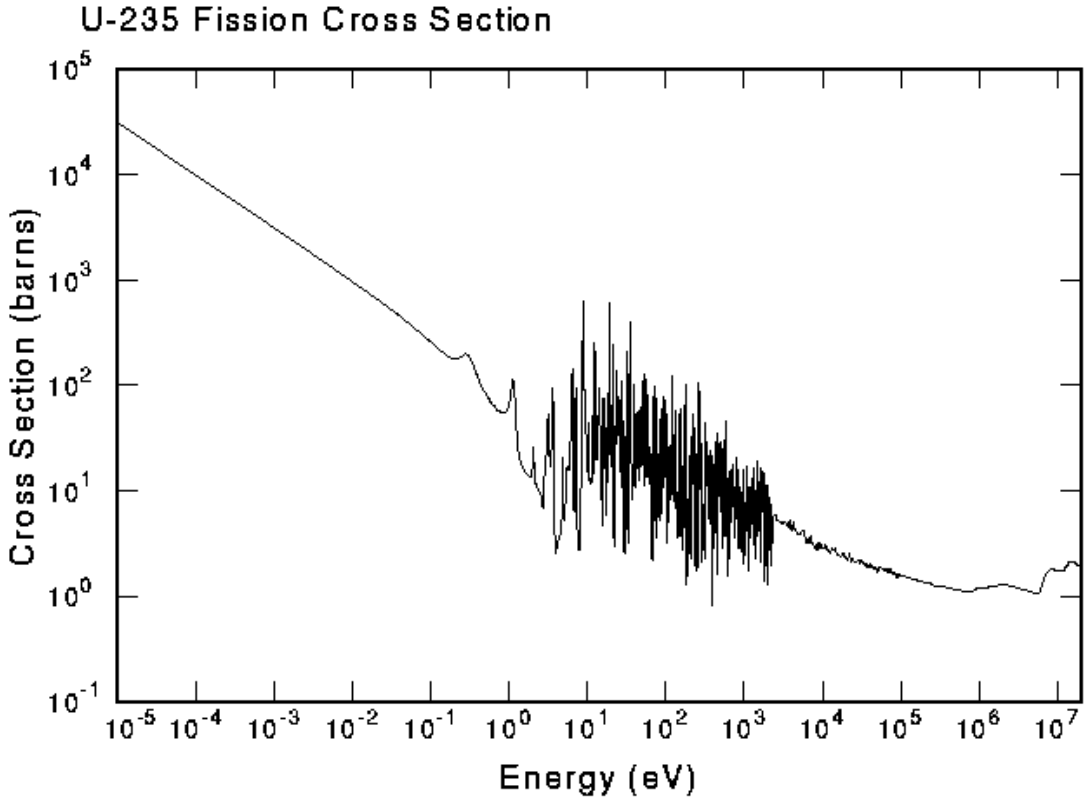

Figure 6. Resonance region of the fission cross section of U-235 [25].

From Figure 6 it is illustrated that for the fission of U-235, the cross section in the thermal energy range is significantly larger than in the resonance energy range and the fast energy range. Here the probability of a neutron being absorbed by U-235 and subsequently fissioning is the largest, and this is why the neutrons are moderated to lower energies.

Light or heavy water is used in most nuclear reactors as a moderator to reduce the energy of the neutrons. The moderator usually also operates as a reflector, reflecting the fast neutrons coming from fission, scattering neutrons back into the active core and increasing the neutron economy.

HEAT AND THERMAL HYDRAULICS

Heat is defined as a form of energy that is transferred from one system to another as a result of temperature difference. Hydraulics is explained as the mechanical properties of liquids, whereas thermal hydraulics studies the liquids in a flowing regime [26]. Thermal hydraulic analysis involves many steps, and can be defined in different ways with respect to the problem at hand. Thermal hydraulic calculations can be used to determine the heat transfer between a heat source and receiving medium, it can determine resistances and temperature distributions, and it can determine the heat transfer coefficients and the thermal conductivities of a system [27].

Finding the heat transfer coefficient, h, is of paramount importance. The coefficient explains the heat transferred between the heat source and the heat receiving medium surrounding the heat source, i.e. the environment. The heat receiving medium is here referred to as the fluid. The h is a part of *Newton's law of cooling* [28], represented in (2)

$$Q = h \cdot A \cdot (T_s - T_b) \tag{2}$$

This is the general form of Newton's law where Q is the total heat generation, T_s is the temperature of the surface of the heat source, T_b is the temperature of the environment, or bulk, and A is the surface area of the heat source. To calculate the specific h value from an individual heat source to the surrounding fluid, the total heat generation can be reduced to the heat generation per heat source. This is shown in (3).

$$\bar{q} = h \cdot (T_s - T_b) \tag{3}$$

The heat capacity law is another way to present Newton's law of cooling [23]. It contains properties of the flow regime of the fluid transporting the heat, and also intrinsic values of the fluid. The temperature difference present in the

heat capacity law deals with the temperature of the outlet and the inlet of the system, and not the temperature at the surface of the heat source and the bulk of the fluid which (3) does. The heat capacity law is presented in (4).

$$P = (T_{out} - T_{in}) \cdot \dot{m} \cdot c_p \qquad (4)$$

where T_{out} and T_{in} is respectively the temperature of fluid exiting the system and entering the system and $\dot{m}$ is the mass flow rate of the fluid, given in kilograms per second. c_p is the specific heat capacity of the fluid. The P is here evaluated for the whole system, and is thus the rate of the total amount of generated heat. The equation is manipulated to contain other variables and is stated in (5).

$$P = (T_{out} - T_{in}) \cdot \left(\rho \cdot \dot{V} \cdot c_p\right) \qquad (5)$$

where $\dot{m} = \rho \cdot \dot{V}$. When the volumetric rate of the fluid is known, it is more convenient to replace the mass flow rate with the density,ρ, and the volumetric flow rate, G. (5) is used in the extrapolation of the modelling, together with (3).

Heat transfer is by convection when the fluid is in motion and by conduction when the fluid layers are stationary [27]. Heat transfer in a stationary fluid is (when neglecting radiation) determined solely by conduction, and is given by *Fourier's law of heat conduction* [28], which is represented in (6)

$$\dot{Q}_{cond} = -k \cdot A \cdot \frac{dT}{dx} \qquad (6)$$

where A is the surface area of the heat source and dT/dx is the temperature gradient. The negative sign is included due to heat always being transferred in direction of decreasing temperature.

For a heat generation system with cylindrical geometry, the heat transfer from the centre line to the outer surface of the cylinder will need to be solved for a radial profile. Using Fourier's law from (6), the radial temperature profile can be determined by using cylindrical coordinates, which is shown in (7).

$$-q'''(r) = \frac{1}{r}\frac{d}{dr}\left(k(r) \cdot r \cdot \frac{dT(r)}{dr}\right) \tag{7}$$

where the q''' stands for the volumetric heat generation, the negative sign symbolizes that heat is transferred to areas with the lowest temperature, and $k(r)$ is the radially dependent thermal conductivity. The thermal conductivity is radially dependent since the temperature changes with respect to the position in the cylindrical geometry.

The heat transfer coefficient can be found through a parameter without dimensions called the *Nusselt number, Nu*. The Nusselt number, given in (8), attempts to characterize the conditions of heat transfer for various geometries and flow conditions for conductive and especially convective heat transfer. The use of a Nusselt number is a common practice in convection studies [28].

$$Nu = \frac{h \cdot L_c}{k} \tag{8}$$

where k is the thermal conductivity of the fluid and L_c is the characteristic length of the heat source. The characteristic length of the heat source depends on the shape of the heat source.

Figure 7 shows an axial slice of a specific geometry of two concentric cylinders with heated cylinders placed between the outer and inner cylinder, similar to the JEEP II fuel element geometry.

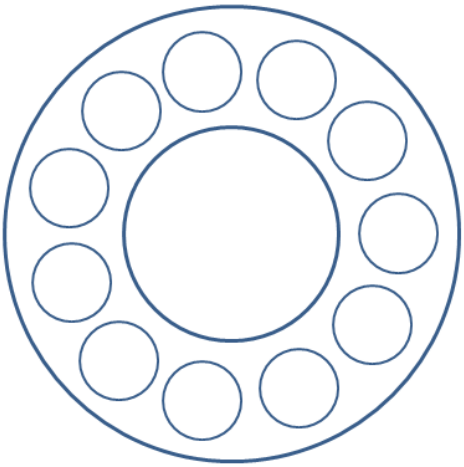

Figure 7. *Possible geometry for heat transfer, where the heated surfaces are within two concentric cylinders.*

For the specific geometry of Figure 7, the characteristic length is replaced with the hydraulic diameter [29]. The hydraulic diameter is expressed in (9).

$$D_h = \frac{4 \cdot A}{W} \tag{9}$$

where A is the flow area surrounding the fuel rods within a fuel element, and W is the *wetted perimeter*. The wetted perimeter is the length of the surface area in contact with the flow, or the perimeter of the cross sectional area that is in contact with the flow.

THE NUSSELT NUMBER

Dividing heat transferred by convection by heat transferred by conduction results in the Nusselt number [26]. The larger the Nusselt number, the more effective the heat transfer by convection. Finding the heat transfer coefficient through (8) is a straightforward calculation, but finding the Nusselt number for a specific flow regime and different geometries is a harder task. Several correlations can be found for different geometries, all of them varying greatly and including uncertainties [30].

General Nusselt correlations include the *Prandtl number* and the *Reynolds number.* The Prandtl number describes the relative thickness of the velocity boundary layer and the thermal boundary layer, and is comprised of the thermo physical characteristics of the fluid [28]. The Reynolds number describes the flow regime, and is given as the ratio of the inertial forces to viscous forces [28]. The flow can be laminar or turbulent, where laminar flow is characterized by smooth streamlines and highly ordered motion, and turbulent flow is characterized by velocity fluctuations and highly disordered motion. A turbulent flow greatly enhances the heat and momentum transfer between fluid particles, which also results in increased friction force on the surface and increased convective heat transfer rate [28]. While enhanced heat transfer is preferred in hydraulic design, the increased friction force leads to a pressure loss in the system and a larger pumping capacity is usually needed.

In finding the Prandtl and Reynolds number for a moving fluid in a system, several thermo physical properties are necessary. Specifying the fluid as heavy water, the values are found in scientific tables [31]. Properties needed for the Prandtl number and Reynolds number are the following: density, specific heat capacity, thermal conductivity and dynamic viscosity. These values are tabulated for certain temperatures, and these temperatures do not always correspond with the temperature that is present in the core. The values from the table containing the properties of heavy water are not tabulated with a resolution of 1, so in many cases interpolation is necessary.

The heat transfer values vary greatly in the entrance region for the heavy water, i.e. the region where the velocity and temperature profiles are still developing [29]. The profiles of the temperature and the velocity can be neglected if the entrance region only is a small percentage of the whole flow channel. For a Prandtl number of over 1, the turbulent region governs the flow regime, making the laminar layer very thin. The boundary layer can for conditions such as these be neglected [29].

BOILING (ACCIDENT SITUATION)

In a typical nuclear reactor, in bad accidents very high temperatures may lead to a vapour blanket layer forming at the cladding. An excursion of the surface temperature happens due to departure from nucleate boiling (DNB), shown in Figure 8 as the transition from point C to point C' [29]. A design limit in nuclear technology is the *critical heat flux* (CHF) [29]. The departure from nucleate boiling comes in to force when the critical heat flux is reached. This means that the vapour coating at the surface of the cladding of the fuel hinders the contact between the water and the cladding. The heat transfer capability of water is then quickly exchanged with a blanket of water vapour, a poor substitute. The sudden deterioration of the heat transfer leads to a jump in the temperature of the cladding, and when the temperature reaches a certain level it is possible to begin melting the fuel rods [4].

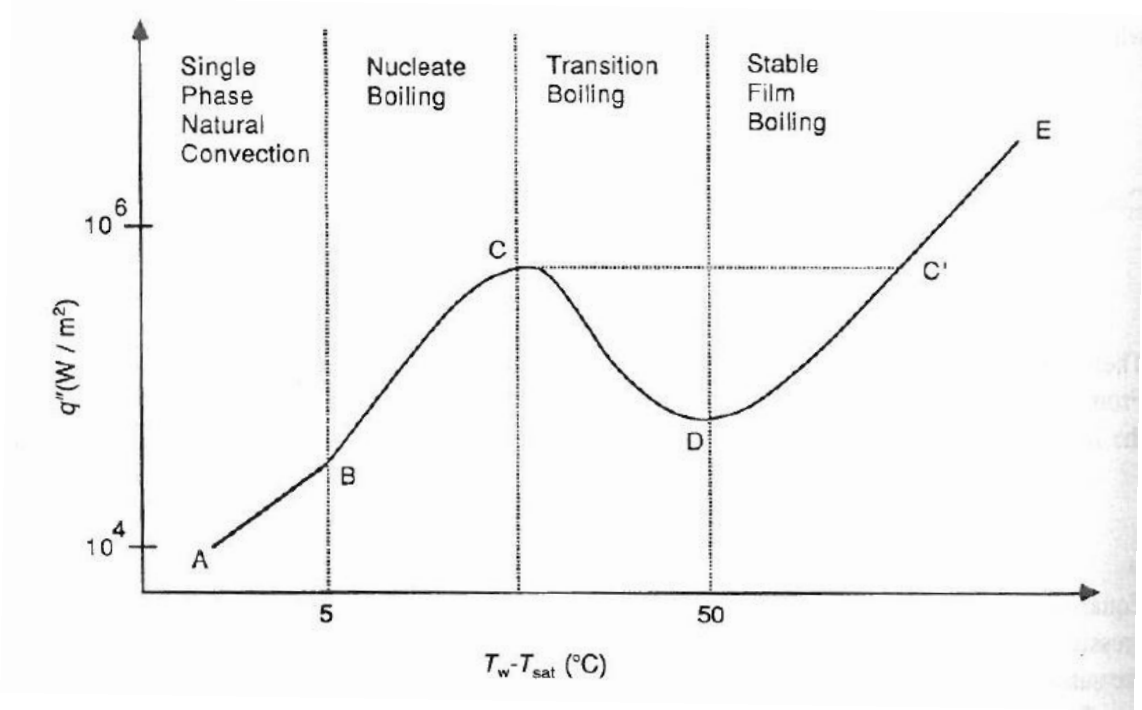

***Figure 8**. Nukiyama pool boiling curve* [7] *that illustrates the relationship between temperature and heat flux and the departure from nucleate boiling* [29].

The departure from nucleate boiling is as shown in Figure 8 where there is a sudden increase in temperature while the boiling regime goes from nucleate boiling to stable film boiling. The straight line between C and C' illustrates the departure. The CHF is the value of the flux at the point C.

Nucleate boiling is a very effective way of transferring heat, and is in fact desired in many reactors [23]. The departure from nucleate boiling gives a sudden increase in temperature at the cladding surface while the regime of the water changes from nucleate boiling to stable film boiling [7]. DNB only happens in a severe accident situation, but must be included as a part of the design-basis of all reactors [32].

4. Method

Schematics and data

The primary main coolant circuit

The circuits are divided in to three main groups: D_2O-circuits, H_2O-circuits and gaseous circuits [33]. The heavy water circuits cover inter alia the primary main coolant circuit and the backup coolant circuit. The primary main coolant circuit removes the generated heat from the fuel pins to the secondary main coolant circuit through a heat exchanger. The backup coolant circuit removes the decay heat in the case of a failure in the primary main coolant circuit.

This thesis only covers the heat transfer in the fuel pins and the surrounding heavy water; however, an insight in how the heavy water circulates through the primary circuit and deposits the received heat from the fuel pins is of interest. Figure 9 shows the schematics of the reactor tank and the primary main coolant circuit including the two heat exchangers HEA 1.1/1.2, the primary main coolant circuit pump PuA 1.1 and the backup pump PuA 1.2.

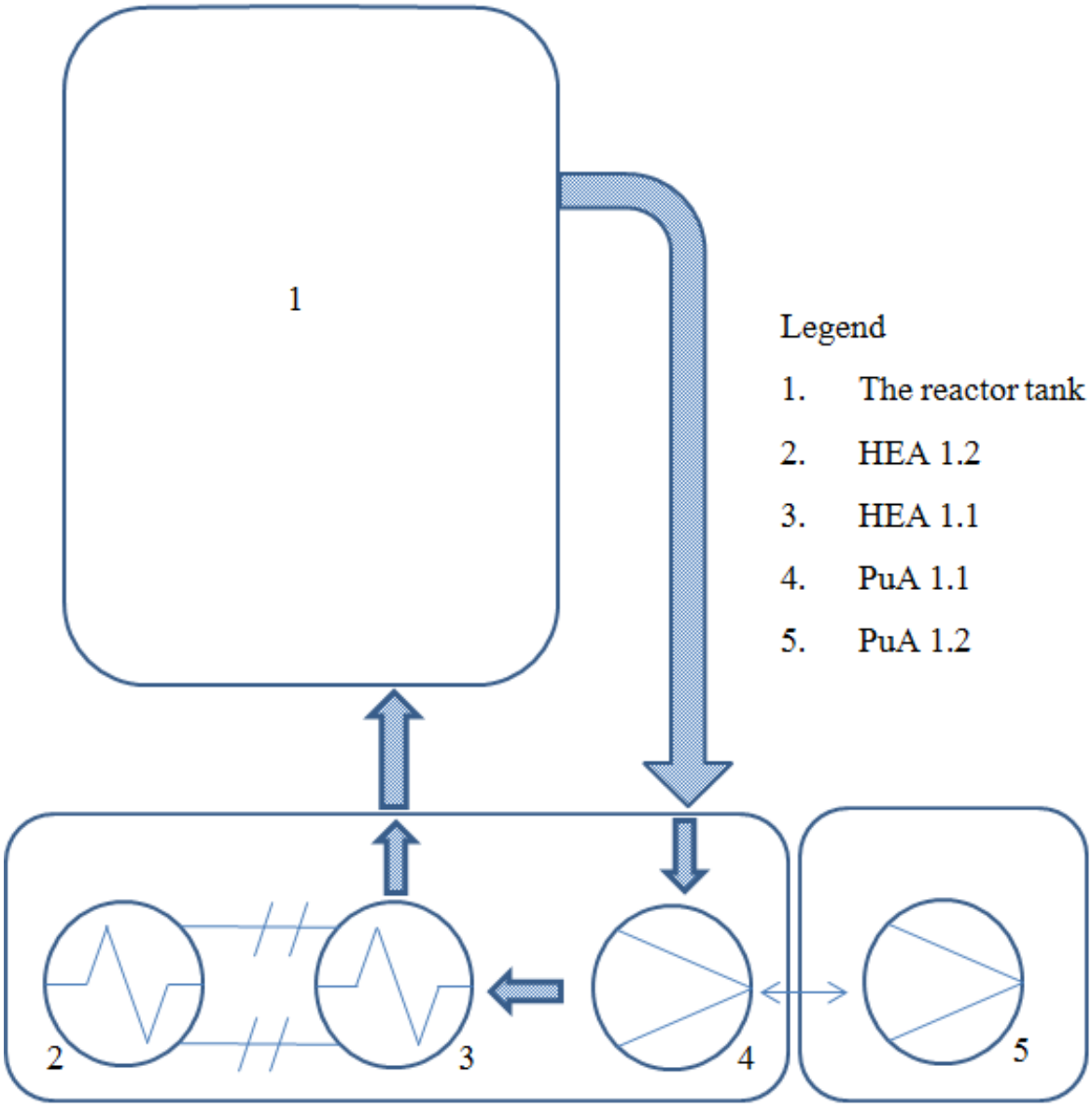

Figure 9. *Schematics of the primary main coolant circuit including the core, the two heat exchangers HEA 1.1 and HEA 1.2 working in parallel, the primary main pump PuA 1.1 and the backup pump PuA 1.2.*

Flow scheme

Heavy water is contained within the primary main coolant circuit, and operates as the reflector, the moderator and the coolant. The reactor core contains around 80 % of the total amount of coolant in the primary main coolant circuit, i.e. 4 out of 5 metric tons [33]. The circulation in the primary main coolant circuit is driven by a centrifugal pump, the primary pump PuA 1.1, with another pump, PuA 1.2, in backup coupled in series with PuA 1.1 [33]. The flow chart of the primary main coolant circuit can be described as follows:

The heavy water circulates from the distributing room below the reactor tank and up through the fuel elements in the core. Most of the flow travels along the 11 fuel pins in the shroud, leaving around a tenth of the total flow through an element through the centre tube [33]. The heavy water can leave the element either through holes in the side, or through the centre tube at the top. A sketch of the fuel element is given in Appendix A3. The heavy water exits the core in the outlet pipe, and enters the heat exchanger room where the main components of the primary circuit are located. The water is pumped by the main pump to the two main heat exchangers HEA 1.1/1.2, and further on to reach the distributing room under the reactor tank. The volumetric flow rate in the primary main coolant circuit is 235 m^3/h, with a pressure difference of 0.14 MPa over the pump. This gives a temperature decrease of 6.15 °C over the heat exchangers, at a reactor power of 2 MW [33]. At 2 MW conditions, which are the normal operating conditions for JEEP II, the heavy water temperature is 56 °C prior to entering the heat exchangers and 6.15 °C lower after exiting.

The core

The active core of the reactor is located in the reactor vessel. The heavy water inlet is pumped in to the centre of the tank, so that the water can be distributed to all the elements. The outlet of the heavy water is located 10 cm

below the top of the active part of the fuel length. The width of the reactor tank is 170 cm at the bottom, and 184 cm at the top and the height is 340 cm [33]. In the core, there are a total of 51 vertical positions arranged in a triangular lattice with a mesh distance of 10 cm. 45 of the positions are designed to contain the fuel elements and channels for experiments, while the remaining 6 positions are designed for the control rods. Under normal operating conditions, the core comprises of 19 fuel elements arranged in a triangular lattice, with a fuel pitch of 20 cm [33]. The core layout with the 19 fuel elements is shown in Figure 10.

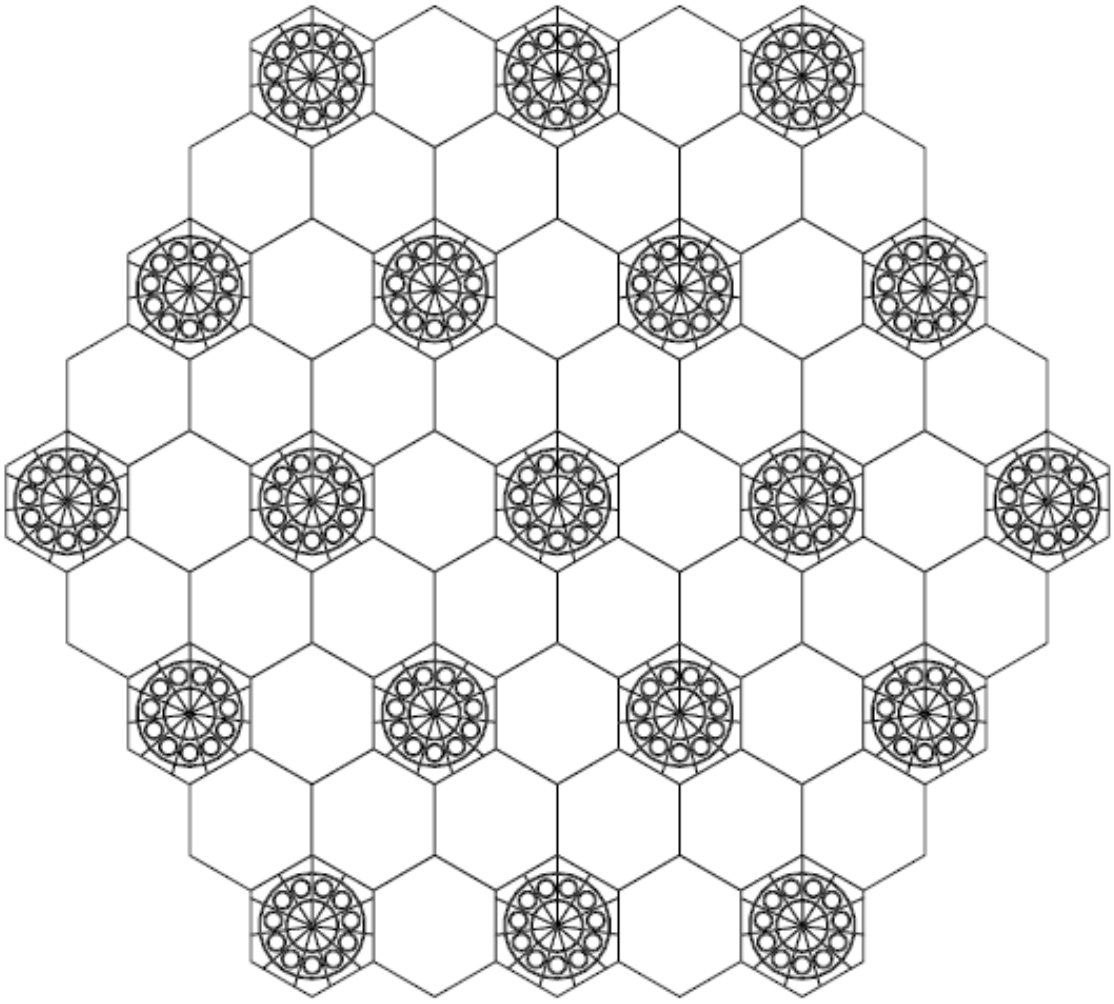

Figure 10. *Cross section of the hexagonal structure of the core with the 19 fuel elements* [34].

The fuel part of the fuel element is contained within two concentric tubes; this is referred to as the inner and outer shroud. The outer shroud has a diameter, d_o, of 87 mm, whereas the inner shroud has a diameter of 41 mm. Within the outer aluminium tube and the inner aluminium centre tube, 11 fuel pins are placed in a circle. The inner and outer shroud combined, i.e. the outer cylinder, the inner cylinder and the 11 fuel pins is referred to as the shroud. The 11 fuel pins are in a symmetrical position with respect to the centre axis of the fuel element [33]. A cross section of the shroud with the 11 fuel pins and an axial view of a fuel pin are given in Figure 11.

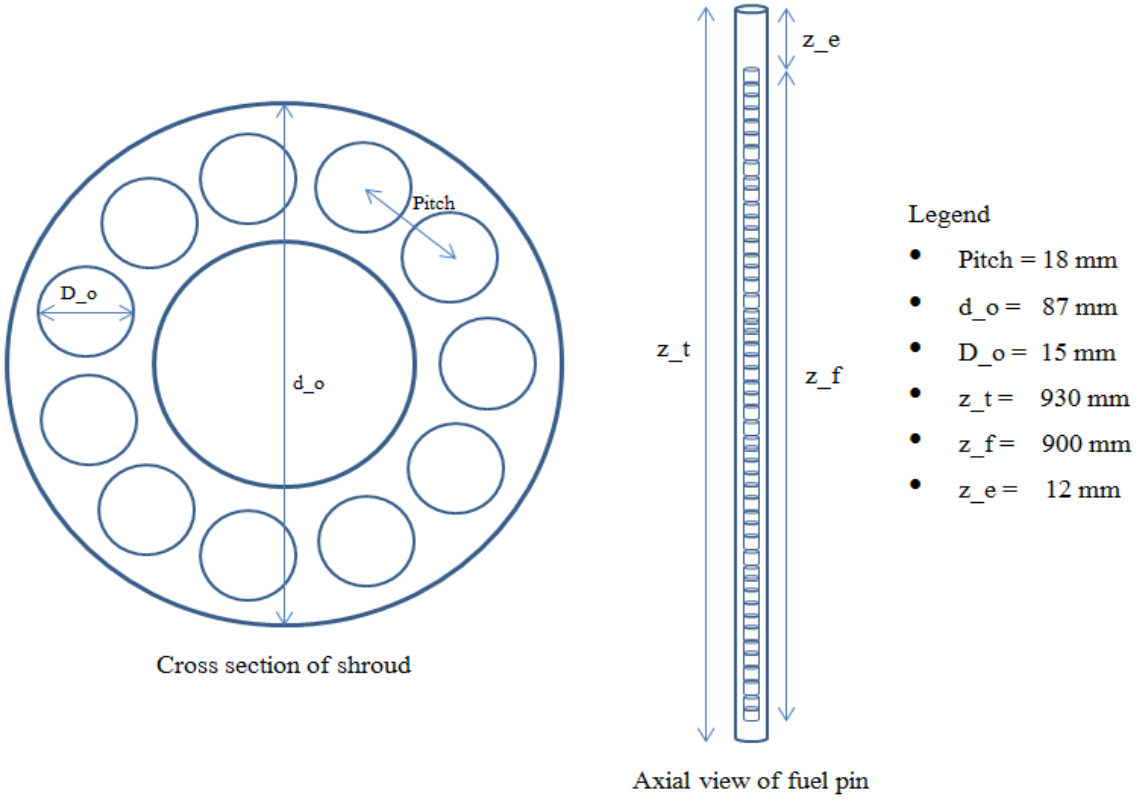

Figure 11. *Cross section of the shroud and an axial view of a fuel pin.*

A known nuclear term is the pitch-to-diameter ratio, where the pitch is the linear distance from the centre of a fuel pin to the centre of the nearest neighbour fuel pin [29]. The pitch for two fuel pins is 18 mm, and the outer diameter, D_o, of a fuel pin is 15 mm; resulting in a pitch-to-diameter ratio of

ca. 1.2. The total length of a fuel element is 1 496 mm. An overview of the fuel element is given in Appendix A3.

Each fuel pin has around 50 uranium dioxide (UO_2) cylindrical fuel pellets inside with a diameter of 12.8 mm. The total length, z_t, of a fuel pin is 930 mm, whereas the total length, z_f, of the fuel pellets is 900 mm, also referred to as the active length. The total amount of fuel in all of the fuel pins is around 250 kg of UO_2, enriched to a U-235 grade of 3.5 % [33]. Between the plug that seals the top of the fuel element and the highest placed fuel pellet, there is a void, z_e, of 12 mm to compensate for potential thermal expansion of the fuel and fission gas release. The fuel pin is filled with helium at a pressure of 1 bar. The helium-gas is between the inner surface of the cladding, and the outer surface of the fuel pellets; a 0.2 mm gap.

Empirical values

IFE's internal Safety report from 2011 includes measurements and calculations done on the core [33]. A conservative approach is also here taken in calculating the temperatures of the fuel pins. Measurements done in a BWR with heavy water as the moderator and coolant show a maximum centreline temperature of the fuel pellets at just below 1 000 °C [33]. These measurements are comparable with the JEEP II reactor because of the similarities in flow conditions, coolant and geometry. Both the measured and calculated values follow in Table 1.

Table 1. *Average and maximum temperatures of a fuel pin in the JEEP II reactor, both measured and calculated.*

	Value
Temperature of coolant inlet/°C	50
Temperature of coolant outlet, mean/°C	62
Decrease in temperature cladding/coolant, mean/°C	25
Temperature decrease cladding/coolant, maximum/°C	50
Decrease in temperature cladding, mean/°C	1.1
Decrease in temperature clad, maximum/°C	2.2
Clad temperature, mean/°C	78
Clad temperature, max/°C	111
Decrease in temperature helium gap, mean/°C	130
Decrease in temperature helium gap, max/°C	266
UO_2 surface temperature, mean/°C	197
UO_2 surface temperature, max/°C	366
UO_2 centre temperature, mean/°C	622
UO_2 centre temperature, max/°C	1 228

Some of the data were determined conservatively, e.g. the heat conductivity for the uranium dioxide fuel pellets. In Table 2, the specifics of the JEEP II reactor at nominal power are listed, including inter alia the heat transfer coefficient of the helium gap, the thermal conductance for the uranium oxide fuel pellets, the heat conductance for the aluminium cladding and the heat

transfer coefficient for the junction cladding/heavy water. Some of the specifics are measured under operation, and some values are calculated.

Table 2. *Specifics of the fuel pin, including inter alia heat transfer coefficients and flux.*

	Value
Heat transfer coefficient of helium in gap/(W/(m^{2}K))	2 000
Heat transfer coefficient at the cladding/(W/(m^{2}K))	9 200
Thermal conductance for UO_2/ (W/(mK))	2
Heat conductance for Al/ W/(mK)	221
Reactor power/MW	2
Power per element, mean/kW	105
Specific load, mean/(kW/kg)	7.9
Power density, mean/ (kW/litre)	3.5
Heating surface per element/ cm^2	4 665
Heat flux at cladding surface, mean/ kW/m^2	226

The values in Table 2 are compared with the results from the 2 MW model, to verify its validity. Average values are used for the thermal conductance coefficients of UO_2 and aluminium.

Modelling the 2 MW JEEP II Reactor

The focus of the modelling of the 2 MW JEEP II reactor will be the heat transfer in the fuel pins, and the heat transfer from the fuel pins to the heavy water, i.e. a condensed version of the thermal hydraulics. The modelling is done in Matlab, and this will be referred to as the script. The 2 MW script is attached in Appendix A1. The aim of the 2 MW model is to make the temperatures to be consistent with the empirical values from the Safety report. The process of identifying the temperatures include uncertainties in linearly interpolating the thermo physical properties of the heavy water, in applying Nusselt correlations for the fuel element geometry and coolant flow in the reactor, and in identifying the heat transfer coefficients of the fuel pin. Ultimately the comparison with the empirical values from the Safety report is the basis for verifying the model. The uncertainties are therefore mentioned, but not assessed.

Assumptions

Before modelling the 2 MW case of the JEEP II reactor, some assumptions were taken, based on the conservative approach of the assignment and the nominal operation of the reactor. It is assumed:

- A continuous velocity distribution of the heavy water within the shroud. This means that there is no sudden acceleration or deceleration of the water on its way from the entrance region and through the shroud.

- That this is a single phase heat transfer problem, i.e. the heavy water is always at its liquid phase

- That the shroud surfaces are smooth. A smooth surface of the shroud decreases the friction between the tube walls and the heavy water flowing along [6]

- That the flow of the water has been fully developed while flowing along the active parts of the fuel pins. A fully developed flow means that the thickness of the thermal and velocity boundary layers is constant.

- A heat generation rate following a cosine distribution. This is due to the fact that the axial thermal flux shape over a fuel pin can be assumed to follow a cosine shape, leading to the heat generation rate also following this distribution [29]. This cosine distribution is assumed to have a constant shape from the fuel element surface to the centre of the fuel pellets.

- That there is no heat transport in the axial direction. For a fuel pin of a length-to-diameter ratio of more than 10, it is safe to neglect the axial heat transfer within the fuel relative to the radial [29]

- An inlet heavy water temperature of 50 °C and an outlet heavy water temperature of 56 °C [33]

- The effect of the control rods on the flux shape is neglected

- Average thermal conductivities

The geometry of the core sets the standard for how the heavy water flows through. From IFEs Safety report the dimensions of a fuel element are given, including the length of one fuel pin, the inner and outer diameter of a fuel pin and a fuel element and the diameter of a fuel pellet. With these dimensions, a fuel element can be modelled in the script.

NUSSELT CORRELATIONS

Finding the Nusselt number leads to the heat transfer coefficient, which is, as previously mentioned, an indication on the amount of heat transferred either by convection or conduction. The Nusselt number can be found through different correlations, all varying greatly depending on inter alia the flow and

the geometry. All the correlations include the Reynolds number and the Prandtl number, and this is therefore a good place to start.

The Prandtl number requires specific information of the fluid, thus some values are needed before computing it. The mechanical characteristics of the fluid, i.e. the dynamical viscosity, the specific heat capacity and the thermal conduction coefficient of heavy water at a heavy water temperature of 56 °C, are found in tables and were in this case found by linear interpolation. The interpolation from the script is shown below

```
t_k = 50:10:70;
c4 = [0.618 0.625 0.629]
k = interp1(t_k,c4,x);
```

The example shows an interpolation for the value of thermal conductivity, *k*. Here the temperature interval is between 50 and 70 °C, with a 10 degree step per value of the thermal conductivity. The string c4 containing thermal conductivities must have the same length as t_k, i.e. 3 [35]. There is a corresponding value of the conductivity for each of the three temperatures. The command interp1(t_k,c4,x) executes a 1D linear interpolation in Matlab to find the thermal conductivity at temperature x.

The Prandtl number for the JEEP II 2 MW case is ca. 4.1, where the closer the number is to zero, the more effective the conductive heat transfer is. The Reynolds number requires information of the fluid and the geometry of which it flows through, in other words the velocity, viscosity and density of the heavy water through the fuel channel, and the hydraulic diameter of the fuel channel. The Reynolds number reveals the flow to be turbulent or laminar. In the JEEP II 2 MW case, the Reynolds number is about 27 000, i.e. the flow is turbulent since it is above ca. 4 000 for an assumed internal flow.

Having the Reynolds number and the Prandtl number, the next step is finding Nusselt correlations that can be implemented on the geometry of the fuel element. The heat source is the fuel pins contained within the shroud, as was presented in Figure 7. A total of six different correlations were found so as to make the comparison with the empirical values from the reactor justifiable.

The Markozy correlation is presented below, the other five correlations are found in Appendix A1 and Appendix A2.

The fifth correlation in the script considers fully developed flow along pin bundles, where the bundle is the 11 fuel pins within the shroud. The values of the Nusselt number vary greatly according to the geometry of the pin bundle [29]. It is found that the Nusselt prediction of Markozy are accurate within +- 10 % for a pitch to diameter ratio larger than 1.12 [29]. The pitch to diameter ratio of the pin bundle is ca. 1.2, thus the criterion is met. Markozy [29] developed a correlation for a fuel bundle as a finite array, and this is presented in (10):

$$Nu_{inf} = \phi(Nu_{inf})_{c.t.} \tag{10}$$

where the c.t. stands for a circular tube and the Φ is given as :

$$\Phi = 1 + (0.912 \cdot (Re^{-0.1}) \cdot Pr^{0.4}) * (1 - 2.0043e^{-B})$$

The coefficient B is given by dividing the hydraulic diameter by the actual diameter. The infinite Nusselt circular tube part, Nu_{inf}, from (10) is the Dittus-Boelter equation for heating conditions, a correlation given in Appendix A1 and Appendix A2 as Nu(1). The Markozy Nusselt correlation is in reality the Dittus-Boelter correlation multiplied with the coefficient Φ. It is given in the script as Nu(5).

Finding the temperatures

The thermal flux of the JEEP II varies with respect to position in the core. This is shown in Figure 12. The heat generation is assumed to follow the same shape as the flux; this leads to the assumption that the temperature profile also has this shape. The temperature distribution in the script for the cladding, the gap and the fuel pellets all follow a cosine distribution that peaks at the middle

of the fuel pin. From the JEEP II, the flux has a peak flux shape that is approximately 1.8 times larger at its vertex than at its lowest point at the end of the pin [36]. The axial flux shape in the core in position 52 is calculated using the HELIOS tool, and is presented in Figure 12.

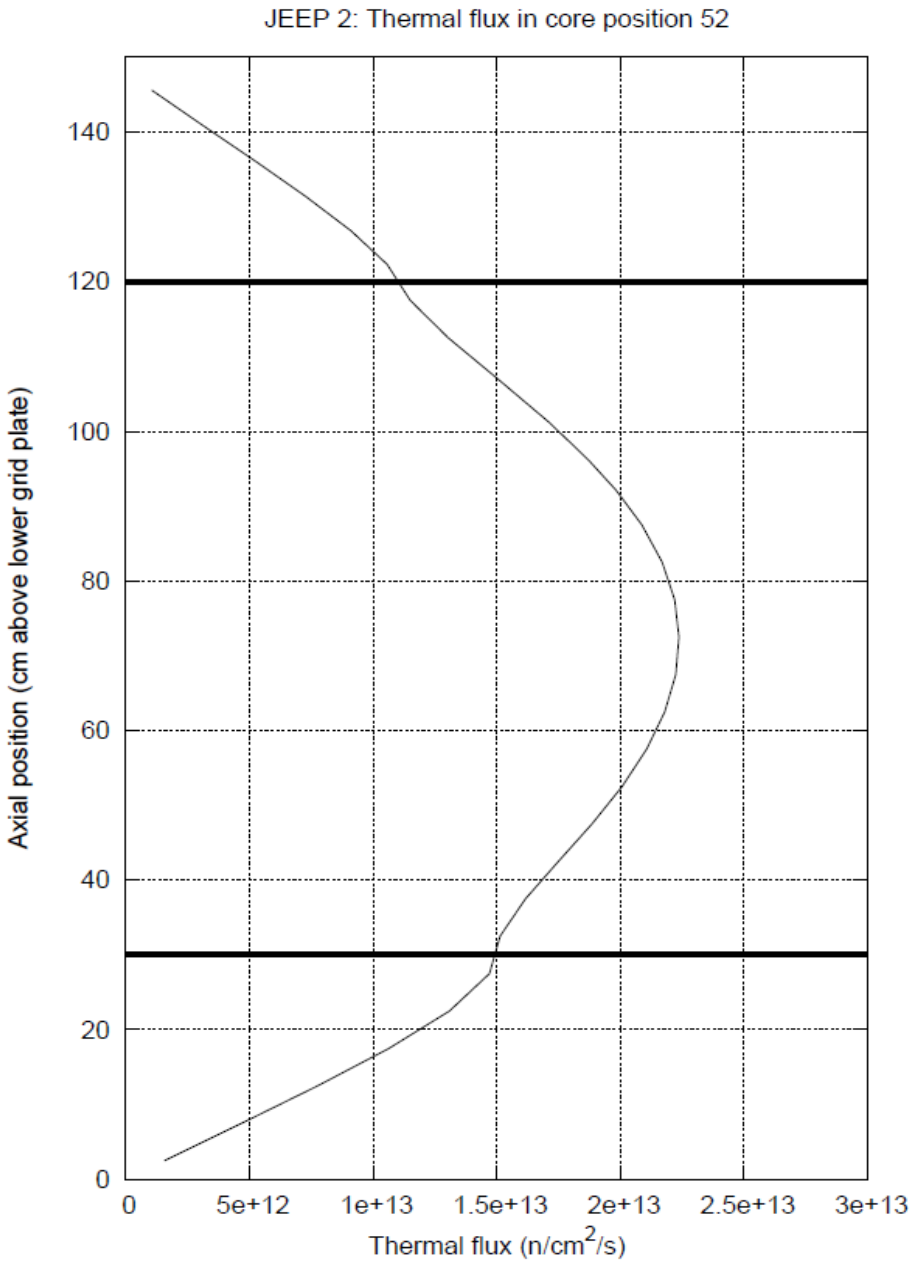

Figure 12. *Axial view of the thermal flux in core position 52, calculated by the HELIOS program* [34].

Figure 12 shows how the vertex point and the low points of the thermal flux in core position 52 differ. This shape is used in the script to create a valid model of the flux and the temperatures, implementing the difference in flux from the vertex to the lowest point. The two highlighted vertical lines represent the lowermost and uppermost parts of the active fuel length of 90 centimetres. The cosine shape is not distributed evenly over the active length of the fuel element; the uppermost part has lower thermal flux than the lowermost part. This probably is a result of the heavy water having a lower density as it receives more heat from the fuel pin, thus having a poorer moderating ability. This is not considered in the script; the endpoints of the fuel pin have the same flux value.

Having gotten six different Nusselt values for the same geometry, (8) is used to get the heat transfer coefficient, with the characteristic length replaced by the hydraulic diameter. The heat transfer coefficient gives a specific value on the rate of energy transferred per area and temperature difference, and is central in the process of calculating temperature distributions in the fuel pin. The six new values of the heat transfer coefficient were arranged in to a vector denoted by b. To calculate the temperatures of the pin from the cladding to the centre of the fuel pellets, a “for”-loop were introduced in the script. A “for”-loop makes it possible to execute a code repeatedly, and can be defined as an iterative statement [37]. For each loop that is executed, one of the six heat transfer coefficients is used to calculate the temperature of the cladding. Below the first lines from the for loop in the script is given.

```
for s = 1:6
        b = [ h(1) h(2) h(3) h(4) h(5) h(6) ];
T_clad = (q_max/b(s)) + T_out
…
…
```

Introducing the “for”-statement gives the loop the command of executing all of the included calculations within the “for”-loop until s is larger than 6. The vector b contains the six heat transfer coefficients, and is used to calculate the cladding temperature. When s is equal to one, the for loop runs what is

included in the for loop for a s value of 1, this is presented in (11)

$$T_{clad}(s) = \left(\frac{q_{max}}{b_1}\right) + T_{out} \qquad (11)$$

Here b_1 is the value of the heat transfer coefficient stemming from the first Nusselt correlation, and q_{max} is the generated heat per fuel pin, multiplied with the hot spot factor of 2.04. At the end of the script, s is changed to continue the "for"-loop, i.e. s = s+1. This is done until s is larger than 6 and the loop closes.

The temperature of the cladding, denoted T_{clad} in the script, is found with (3). The method of the "for"-loop is already shown, the arranging of (3) leading to the cladding temperature being alone at the left hand side is done with two algebraic steps. The T_{clad} is the reference temperature, since it links the conductive heat transfer in the fuel cladding with the convective heat transfer between the heavy water and the fuel cladding [23].

The temperature distribution in the script is a reduced cosine period, i.e. the period of the cosine is reduced to an interval of $-\pi \cdot 0.325 < x < -\pi \cdot 0.325$, with a resolution of 0.01 on the x-axis. This is done so as to make the temperature distribution fit with the heat flux shape from Figure 12. The shape of the temperature distribution is introduced when calculating the heat flux from a fuel pin, and it is presented in (12).

$$q_{z\_v} = \frac{(Q \cdot \cos z\_v)}{N \cdot n \cdot pi \cdot D_o \cdot z\_s} \qquad (12)$$

where D_o is the outer diameter of the fuel element, N is the number of fuel elements and n is the number of fuel pins per element. z_s is the constant value of the length of the fuel pin, and z_v is the vector value of the length of the fuel pin with a resolution of 0.01. This leads to the heat flux having 205 values over the active length of the pin. The temperatures of the cladding and further in to the centre line is calculated with the cosine shape, and is reliant

on array operators in the script. Due to this, each time the cosine shape is a part of an equation, a dot, (.), is inserted in front of the multiplier or division symbol [38].

By finding the thermal conductivity of aluminium and including the aforementioned temperature of the clad, the inner temperature of the cladding can be found. The cladding is made of aluminium, thus the heat transfer is by conduction. Fourier's law of heat conduction, given in (6), can be changed to be valid for heat transfer in a cylinder, by first separating the variables and then integrating from the inner surface to the outer surface of the cladding [28]. Fourier's law of heat conductance has now been altered to contain a heat source part, a temperature difference part and a resistance part, this alteration is presented in (13).

$$T_{cladinside} = T_{clad} + \frac{\left(\log\left(\frac{D_o}{D_i}\right) \cdot Q \cdot Pf \cdot \cos z\_v\right)}{N \cdot n \cdot 2\pi \cdot z\_s \cdot k_{al}} \tag{13}$$

where $D_o$and $D_i$are the outer and inner diameter of the cladding, respectively. The Pf is the hot spot factor of 2.04, to correct for the thermal flux distribution, the position of the control rods, the local peak flux factor and the power overshoot. The thermal conductivity of aluminium is given as k_{al}.

Being at the inner surface of the cladding, the next step is calculating the heat transfer across the gap of the helium gas. This gap is very thin, only about 0.2 mm, but it has a large temperature difference. The helium gas is between the inner surface of the cladding and the outer surface of the uranium oxide fuel pellets. The equation for the heat transfer across the gap is presented in (14) [6].

$$\Delta T_{He} = \frac{Q \cdot Pf \cdot \cos z\_v}{N \cdot n \cdot \pi \cdot d_m \cdot z\_s \cdot h_{He}} \tag{14}$$

where the d_m is the average diameter of the helium gap, and h_{He} is the heat transfer coefficient of the gap. (14) is similar to the altered Fourier formula of (13), but here the heat transfer is by convection. It includes a heat transfer part by convection for a stationary gas, and includes only an average of the diameter of the gap. It gives the difference in temperature through the gap by dividing heat generated per fuel pin and area on the heat transfer coefficient of helium.

Having the temperature difference of the helium gap, it is easy to find the surface temperature of the uranium oxide fuel pellets. Adding the temperature of the inner cladding surface with the raise in temperature in the helium gap gives the surface temperature of the fuel pellets. (15) presents this.

$$T_{UO_2} = T_{cladinside} + \Delta T_{He} \tag{15}$$

The radial temperature profile in the fuel pellets can be determined by solving the heat transfer equation from (7) in cylindrical coordinates and integrating from the centre of the pellets to the surface. The thermal conductivity depends on the temperature which changes radially in the pellets. It is assumed that this dependency is rather small, and an average thermal conductivity of 2 W/mK is chosen. The volumetric heat generation from (7) is changed by multiplying it with the area of a fuel pellet. The temperature drop across the fuel pellets is stated in (16).

$$\Delta T_{fuel} = \frac{Q \cdot Pf \cdot \cos z\_v}{4 \cdot N \cdot n \cdot z\_s \cdot \pi \cdot k_{UO_2}} \tag{16}$$

where k_{UO_2} is the thermal conductivity for the uranium oxide of the fuel pellets. The temperature difference is separated and the centre line temperature is isolated at the left hand side in the script. When the centre line temperature is calculated for the respective s-value of the “for”-loop, the value of s changes with s+1, and the “for”-loop runs again until s is larger than 6.

Extrapolation to 5 MW

The 2 MW model was designed so as to fit with the measured values from the internal Safety report from IFE [33]. It is based on thermal hydraulic calculations, and several assumptions were taken to complete these calculations. As in all research, a "hands on" approach with empirical values is preferred, but in the case of the JEEP II at Kjeller the regular operation of the reactor made this impossible. Thus a model of the reactor under normal operating conditions was made. The next step would be, if the values from the 2 MW model were satisfactory, to extrapolate the model to a case where the power was raised to 5 MW. The model is extracted to 5 MW, and the same variables are used, thus the extraction of the model will be referred to as an extrapolation.

The assumptions taken for the 5 MW case are equal to the ones being taken in the 2 MW case, except for the assumption of the outlet temperature. The power of the reactor is increased, and this will also give a larger heat generation. For the calculations on the 5 MW script, it is assumed that a change in the outlet temperature of the heavy water is present, while the volumetric flow rate is left at 235 m^3/s. The 5 MW case will also be analysed assuming that the volumetric flow rate can be varied as is done in calculations in previously published reports at IFE [1]. The inlet temperature is the same as in the 2 MW case; 50 °C. It is also assumed that the total 5 MW is produced by the original geometry, i.e. that the 19 fuel elements with a total of 209 fuel pins can produce 5 MW.

The heat capacity law from (5) is used for the 5 MW case. To find the outlet temperature, the density and the specific heat capacity of the heavy water flowing along the fuel channel are needed. The bulk temperature of the heavy water is identified through iteration. The temperature iteration is carried out by assuming the temperature increase the heavy water experiences when the power is increased to5 MW. Interpolating linearly for the density and the specific heat capacity, the outlet temperature, i.e. the temperature of the heavy water exiting the reactor tank can be calculated.

Having the outlet temperature of the heavy water, this value is used further as the basis for all calculations. This is due to the conservative approach of the thesis, since the outlet temperature is set as the maximum temperature of the water. The new temperature is used in four new linear interpolations, finding a new density, specific heat, dynamic viscosity and thermal conductivity which is given as rhonew, c_pnew, munew and knew in the script. These values make the Prandtl number, and the Reynolds number is calculated from the flow specifics and the geometry of the flow channel. Here and on the calculations are the same for the 5 MW case as the 2 MW case.

Uncertainty

Error analysis is the study and evaluation of uncertainty in measurement [39]. There is no measuring or laboratory work in this thesis, only mathematical modelling, thus a thorough uncertainty analysis is therefore hard to carry out. The modelling effort in this thesis is completed on the basis of a set of input data from the IFE safety report. This involves the geometry of the fuel elements and the fuel pins and the temperatures of the fuel pin and the heavy water, and the uncertainty related to these issues call for a qualitatively discussion of the sensitivity in relation to each parameter. The combined effects when any of these input data are changed have been presented in chapter 5 and discussed in chapter 6, and the overall conclusion has been included in chapter 7. The results coming from the script are compared with the values from the Safety report to check the validity of the model.

5. OBSERVATIONS

THE 2 MW CASE

The heat flux from a fuel pin was found with (12) and is at its vertex at 226 kW/m^2. Multiplying the heat flux per fuel pin with the hot spot factor of 2.04 gives a maximum heat flux which is presented in Figure 13. The peak value of the maximum heat flux is 460 kW/m^2, with a lower maximum heat flux of ca. 240 kW/m^2.

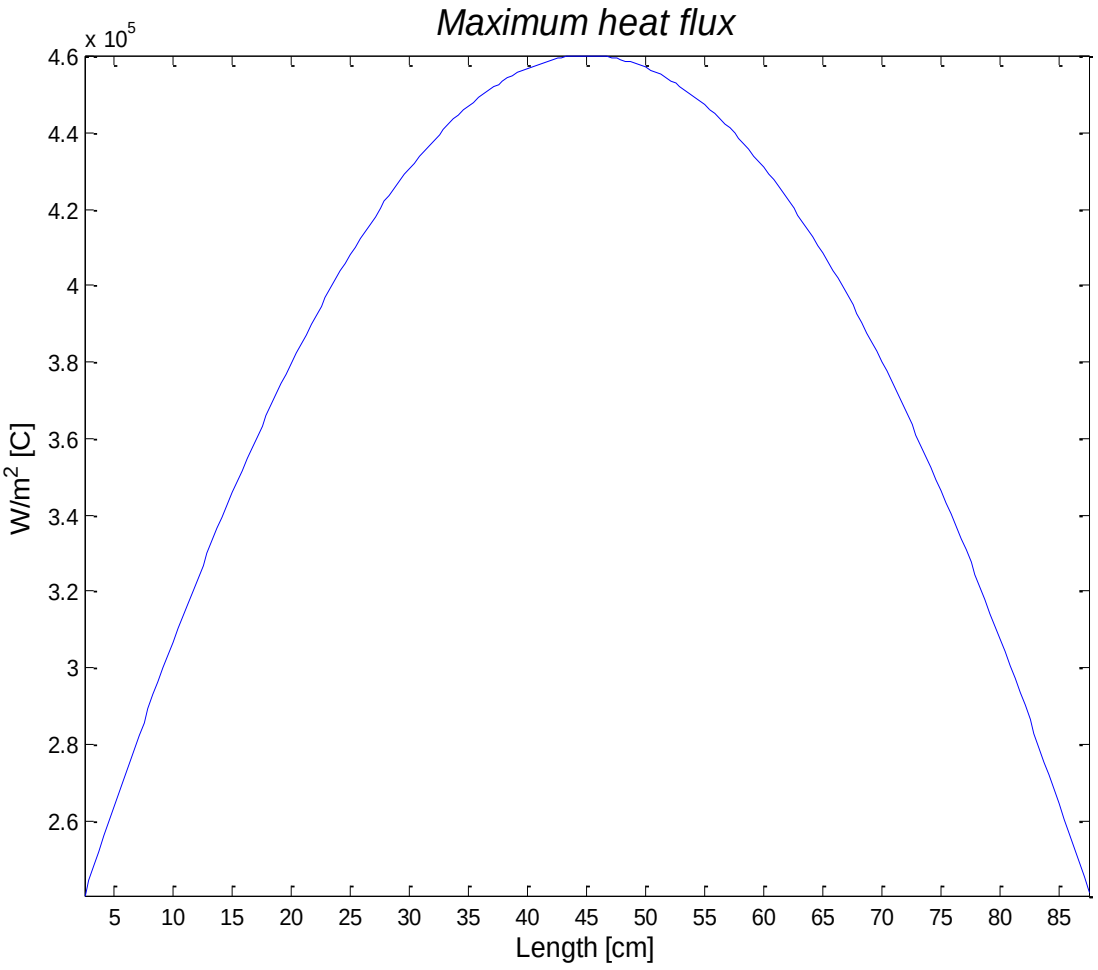

***Figure 13**. Cosine distribution of the maximum value of the heat flux per pin in the reactor for the 2 MW case.*

The maximum heat flux is spanned over the fuel pin with a cosine shape. This is the generated power from the JEEP II divided by the number of fuel pins and their diameter and length, and fitted to the cosine distribution. This is a heat flux of ca. 460 kW per fuel pin per square meter, whereas the measured value from the Safety report gives an average heat flux of 226 kW/m^2 per fuel pin per square meter [33].

The critical heat flux (CHF) of the JEEP II for a power of 2 MW is listed several places, and varies with how conservative an approach taken. The most conservative value of the maximum heat flux found is 0.5 MW/m^2 [7]. A conservative way of evaluating the possibility of reaching the CHF is calculating the critical heat flux ratio, i.e. dividing the maximum heat flux of the reactor with the CHF value from the Zuber correlation for the present pressure [7]. The Zuber correlation gives the conservative value of about 1.5 MW/m^2, yielding a conservative CHF ratio of 3 for the JEEP II at 2 MW. This means that the heat flux can be tripled before reaching its critical value [7]. The critical heat flux ratio is named departure from nucleate boiling ratio (DNBR) in this thesis.

Nusselt numbers and heat transfer coefficients

Five of the six Nusselt correlations lie within a small interval, which gives a good indication on the applicability of the correlations on the JEEP II geometry. The Nusselt number from the Gnielinski correlation is the one value that deviates from the others, and is around 20 % larger than the mean of the other five correlations. The different Nusselt numbers is presented in Table 3.

Further on, the heat transfer coefficient is calculated through the different Nusselt numbers. From the Safety report, the heat transfer coefficient from the cladding to the heavy water is 9.2 kW/m^2K [33]. This measured value should be in compliance with the value from the model to verify the validity of the model. The heat transfer coefficients are given in Table 3.

Table 3. Six different values of the Nusselt numbers and the associated heat transfer coefficients from the 2 MW case.

Nusselt numbers and heat transfer coefficients for the 2 MW modelling		
Nusselt correlation	Nusselt number (dimensionless)	Heat transfer coefficient/(kW/m^{2}K)
Nu(1) - Dittus-Boelter	140	7.5
Nu(2) - Hernes	148	7.9
Nu(3) - Gnielinski	180	9.6
Nu(4) - Pethukov	153	8.2
Nu(5) - Markozy	147	7.8
Nu(6) - Finite array	150	8.0

The most common correlation for heat transfer calculations, the Dittus-Boelter (Nu(1)), has a lower value than the more specific correlations. The Nu(2) is a correlation taken from the IFE report and is named Hernes from the author. The Hernes correlation is used specifically on the JEEP II, and is therefore included in the script. The Gnielinski (Nu(3)) is a general correlation used for flow over circular geometries, as is the Pethukov (Nu(4)). The finite array (Nu(6)) and the Markozy (Nu(5)) are correlations designed for tube banks, fuel pins and nuclear geometries as found in the JEEP II [29]. The latter two are slightly higher than Dittus-Boelter, but together with the other correlations, the deviation from the mean is not large. The mean of the Nusselt correlations is 150.

There are no correlations for the specific JEEP II geometry of a circular fuel bundle within a shroud, but the six Nusselt correlations are chosen for their applicability. The geometry of the fuel bundle is circular, and the fuel pins are cylindrical. The Nusselt correlations deals with flow over a cylindrical geometry, and since the calculations in the script are done for a cylindrical fuel pin the correlations are deemed as applicable. Some of the correlations take into account that the circular geometry is arranged in a bank, as the Markozy and the finite array.

The Gnielinski (h(3)) value of 9.6 kW/m^{2}K is closest to the calculated heat transfer coefficient value from the Safety report ; 9.2 kW/m^{2}K. The average of the heat transfer coefficients from the script is 8.2 kW/m^{2}K .

Temperatures

Executing the “for”-loop for all the different heat transfer coefficients generates plots of the temperatures of the fuel pin. Shown in Figure 14 is a subplot of these temperatures for the Dittus-Boelter correlation. The temperature distribution is at its vertex at the middle point of the fuel pin, and has the lowest values at the uppermost and lowermost parts of the fuel pin. The length of the fuel pin is denoted with “z” in Figure 14. The script calculates the temperatures for the surface of the cladding, the inside of the cladding, the raise over the helium gap, the surface of the uranium oxide fuel pellets and the centre line for the fuel pellets.

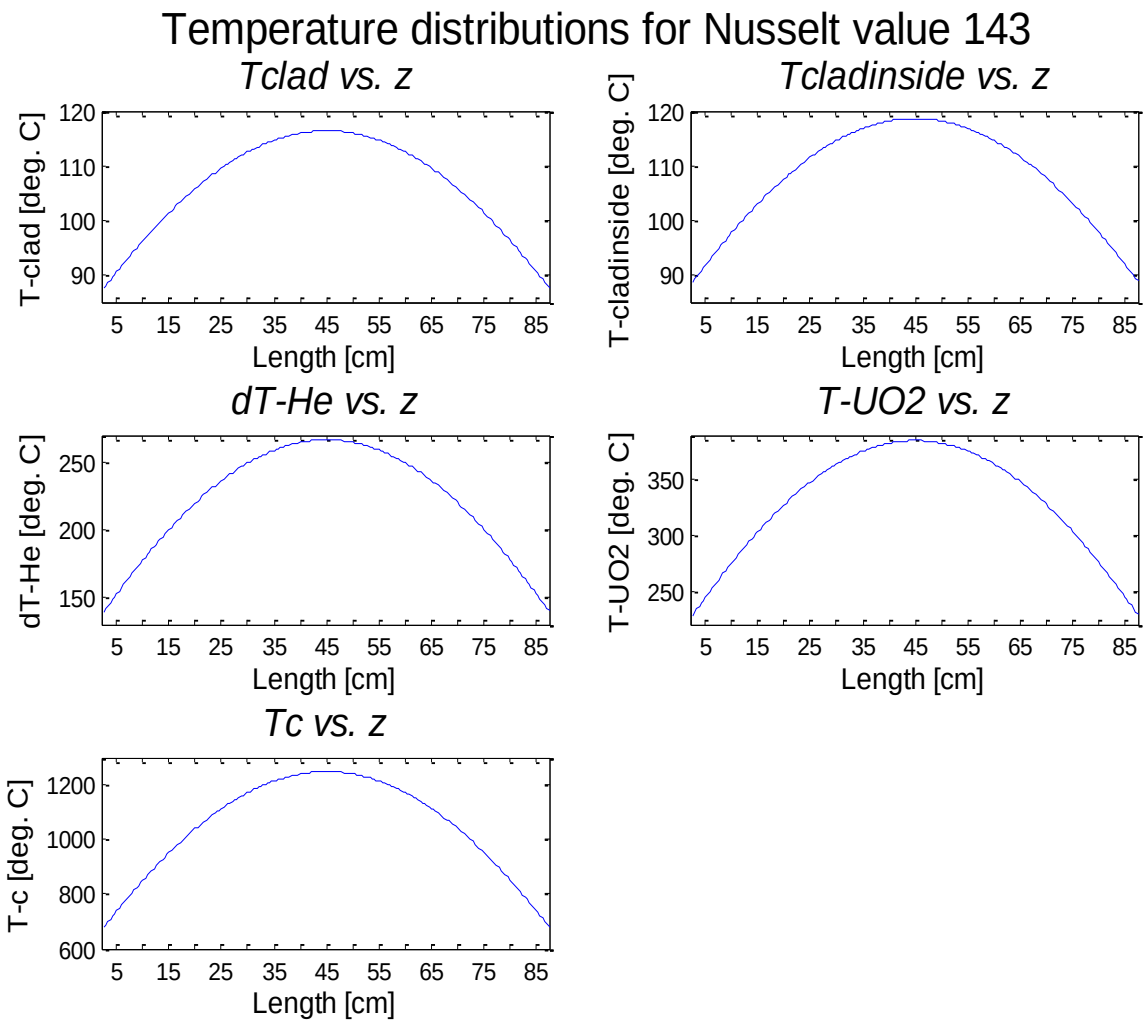

Figure 14 *.Subplot consisting of 5 plots, showing the temperatures from the clad to the centre line of the fuel pellets for the corresponding Dittus-Boelter Nusselt number for the 2 MW case.*

The surface temperature of the cladding spans from 85 °C to a peak of 117 °C, and it is shown in Figure 14 as the subplot with the "Tclad vs. z" heading. The measured temperatures from the Safety report give a mean temperature of the cladding of 78 °C and a maximum temperature of 111 °C. The report also mentions a maximum decrease in temperature from the cladding to the bulk of the water of 50 °C. Further on, the temperature increases inward in the cladding, and the temperature of the inner wall of the cladding is given in Figure 14 as the subplot with the "Tcladinside vs. z" heading. The maximum

temperature increase is rather small; a raise of around 2 °C is present. The Safety report states a maximum raise of temperature through the cladding of 2.2 °C. The subplot “dT_He vs. z” of Figure 14 plots the raise in temperature across the helium gap, which spans from 140 °C to 270 °C. The temperature increases at a maximum value of 270 °C over a gap of 0.2 mm through the inert helium gas. The empirical numbers from the Safety report shows a mean increase of temperature across the gap of 130 °C, and a maximum increase of temperature of 266 °C. Adding the inner wall temperature of the cladding with the raise in temperature over the helium gap gives the surface temperature of the uranium oxide fuel pellets, and this is presented in Figure 14 as the subplot with the “T-UO2 vs. z” heading. The temperatures span from around 235 to 385 °C, whereas the maximum temperature from the Safety report is measured at 366 °C. The temperature in the centre line of the fuel pellets is given in Figure 14 as the subplot with the “Tc vs. z” heading. Here the temperature increases rapidly from the surface to the centre line, peaking at 1 250 °C going down to 690 °C at its lowest maximum value. The Safety report states a mean temperature at the centre line of the fuel pellets at 622 °C, and a maximum temperature of 1 228 °C.

As the Nusselt numbers, except the Gnielinski, are so similar, the values of all the temperatures are within a certain range. For the centre line temperature, the lowest endpoint temperature is 680 °C and the highest vertex temperature is 1 250 °C. Figure 15 shows a column chart containing the six Nusselt numbers, the six temperatures of the cladding temperature, the six temperatures of the inside wall of the cladding, the six temperature increases over the gap of helium, the six temperatures of the surface of the uranium oxide fuel pellets and the six temperatures of the centre line of the fuel pellets. Also included in Figure 15 are the corresponding measured temperatures from the Safety report.

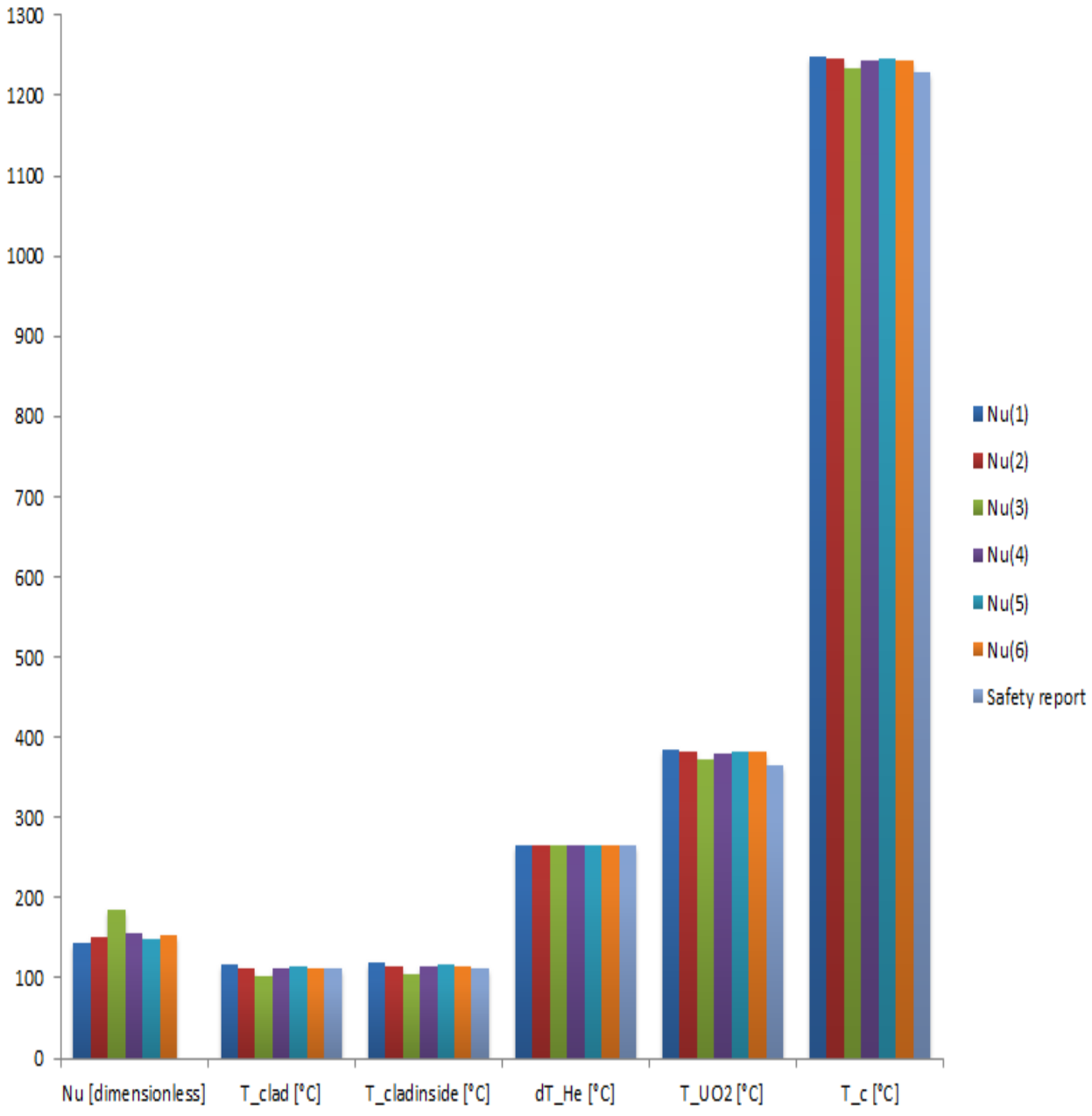

***Figure 15**. Temperatures from the clad to the centre line from the six different Nusselt values from the 2 MW case and the Safety report.*

From Figure 15, it is clear that a larger Nusselt number leads to a lower T_clad and lower temperatures in the fuel pin in general. The Gnielinski correlation, indicated in Figure 15 by the green bar, has the highest Nusselt number and the lowest fuel centre line temperature. The measured and calculated

temperatures from the Safety report, indicated in Figure 15 by the grey bar, is similar to the temperatures from the script, except for the surface of the fuel pellets, T_UO_2, and the centre line temperature, T_c, where it is noticeably lower. The equal increase in temperature across the helium gap comes from the equation being dependent on an isolated heat transfer coefficient of helium, and is thus constant for all the different Nusselt numbers.

VERIFYING THE MODEL

The model was to be verified by the empirical values from the reactor. Several temperature meters, all fairly accurate, are placed in the reactor. From Figure 15 the temperatures from the Safety report are given alongside the results from the model to give a graphical view of the accuracy of the model. In Table 4, the average maximum temperatures from the script and the temperatures from the Safety report are shown.

Table 4. Average maximum temperatures from the script and the measured values from the Safety report.

	T_clad/ °C	T_cladinside/ °C	dT_He/ °C	T_UO2/ °C	T_c/ °C	Heat transfer coefficient/ (kW/m²K)
Average (script)	112	114	267	380	1244	8.3
Safety report	111	113	266	366	1228	9.2

The temperatures do not deviate to a large degree; the largest deviation is at the fuel centre line where the average maximum temperature from the script is 16 °C higher than the measured value from the Safety report, as shown in Table 4. The average of the heat transfer coefficient from the script is a much smaller value than the coefficient from the Safety report, with a deviation of 1.1 kW/m²K.

HEAT FLUX

The power was changed in the script from 2 to 5 MW, while keeping the volumetric flow rate and the inlet temperature at 235 m^3/h and 50 °C, respectively. The change in the power of the reactor leads to changes in the temperatures, Nusselt numbers, heat transfer coefficients, etc. The flux of the reactor increases; it is more than doubled with respect to the 2 MW model. The maximum heat flux, i.e. the power per fuel pin per square meter multiplied with the hot spot factor is given in Figure 16.

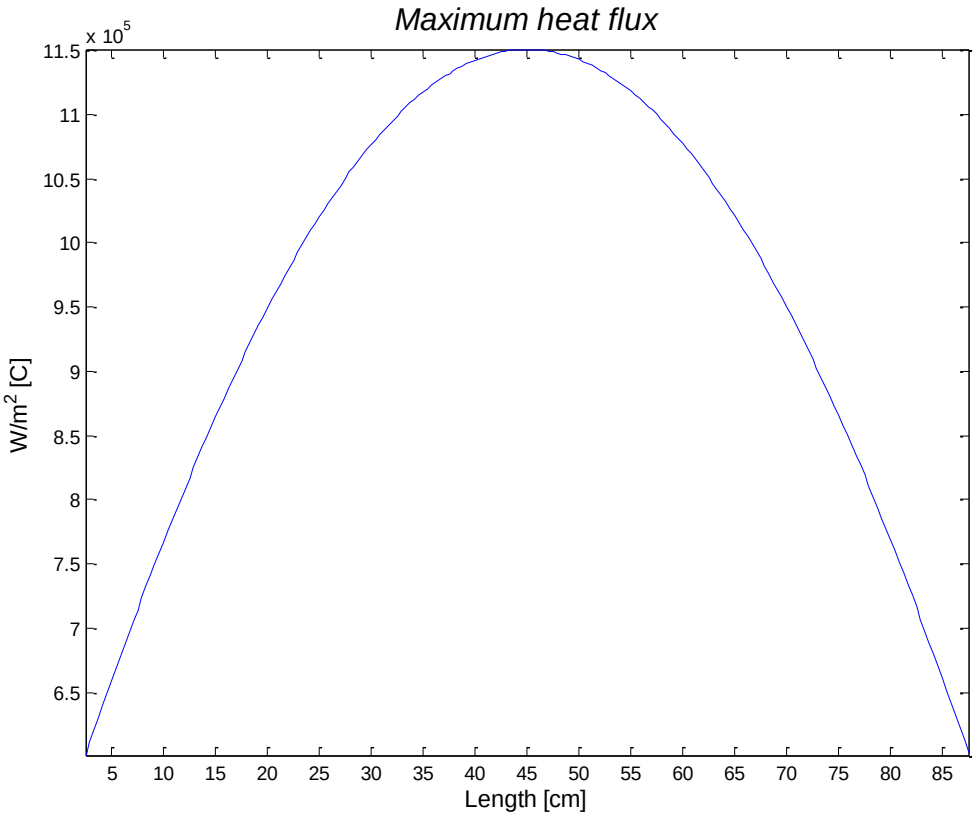

***Figure 16**. Cosine distribution of the maximum heat flux per fuel pin from the 5 MW case*

From Figure 16, the cosine distribution of the maximum heat flux from a fuel pin is presented. It shows a maximum heat flux of around 1.15 MW/m^2 and a

lower maximum level at the edges of the pin of around 0.6 MW/m^2. The DNBR is for the 5 MW case 1.3.

Interpolation

The extrapolation of the model from 2 MW to 5 MW was done with the assumption of an inlet temperature of heavy water at 50 °C. The outlet temperature was to be identified through the heat capacity law from (5). The bulk temperature of the heavy water was identified through iteration, with a temperature range from 50 to 70 °C. Having the temperature of the heavy water, the density and the specific heat capacity was identified through one dimensional interpolation. The outlet temperature could then be identified using the density and specific heat capacity. The text below shows the interpolation for the density from the script.

```
t = 60;

t_rho = 50:2:70;
c1 = [1095.650 1094.691 1093.733 1092.657 1091.703
1090.513 1089.443 1088.258 1087.075 1085.894 1084.716];
rho = interp1(t_rho,c1,t);
```

Guessing the bulk temperature to be equal to the inlet temperature, the temperature of the outlet became 67.018 °C. Guessing a bulk temperature of 60 °C, the temperature of the outlet became 67.103 °C. Guessing the bulk temperature to be 70 °C, the outlet temperature became 67.188 °C. This is only three of the 11 values of the outlet temperature from the iteration, but it shows good agreement. The outlet temperature differs by 0.16 °C while the bulk temperature differed by 20 °C. The bulk temperature of the water did not affect the outlet temperature in a great way in the guess range; demonstrating how small the variation of the thermo physical properties is in this

temperature range. For this reason the temperature was set as the middle point of the iteration temperature range, 60 °C.

Using the new outlet temperature from the interpolation, the density, specific heat capacity, dynamic viscosity and the thermal conductivity is also identified through interpolation. These values are used in identifying the Prandtl and Reynolds number, and then the Nusselt number. As in the 2 MW case, there is six different values of the Nusselt number and the heat transfer coefficient. The same coefficients, friction factor and assumptions are used in this case as for the 2 MW case.

HEAT TRANSFER COEFFICIENTS

The heat transfer coefficients for the 5 MW case is presented in Table 5. Comparing with the Gnielinski(h(3)), the correlation yielding the highest Nusselt number, the value of the heat transfer coefficient has increased from 9.6 kW/m^{2}K to 9.7 kW/m^{2}K. The Nusselt value is calculated with the Prandtl and the Reynolds number, both being dependent on the thermo physical properties of the heavy water. The temperature change is not large, and this results in a small change in the heavy water properties. There is also no change in the geometry of the core or flow of the heavy water. All in all, following from the small change in the thermo physical properties of the heavy water, this leads to a small change in the heat transfer coefficient.

***Table 5**. Six different heat transfer coefficients from the 5 MW case.*

Heat transfer coefficients from the 5 MW modelling	
Nusselt correlation	Heat transfer coefficient/(kW/(m^{2}K))
Nu(1) – Dittus-Boelter	7.5
Nu(2) – Hernes	8.0
Nu(3) – Gnielinski	9.9
Nu(4) – Pethukov	8.2
Nu(5) – Markozy	7.8
Nu(6) – Finite array	8.0

The average value of all the heat transfer coefficients is 8.2 kW/m^{2}K. The only higher value of the heat transfer coefficient for the 5 MW model with respect to the 2 MW model is from the Gnielinski correlation. The thermo physical properties of the heavy water have higher values when the temperature is lower, except for the thermal conductivity. This leads to a higher value for Prandtl and Reynolds, but in the Gnielinski case this gives a higher heat transfer coefficient.

The temperatures

The iteration for the six different values are done with the same principle as in the 2 MW case, there has just been a change in the denotation of the vector that contains the heat transfer coefficients from b to r. High temperatures were expected for the 5 MW case. The fuel centre line temperatures was of importance due to the possibility of reaching the melting point of uranium oxide, and the cladding temperatures was of importance due to the possibility of departure from nucleate boiling. The temperatures stemming from the Dittus-Boelter(h(1)) correlation is presented in Figure 17 as a subplot.

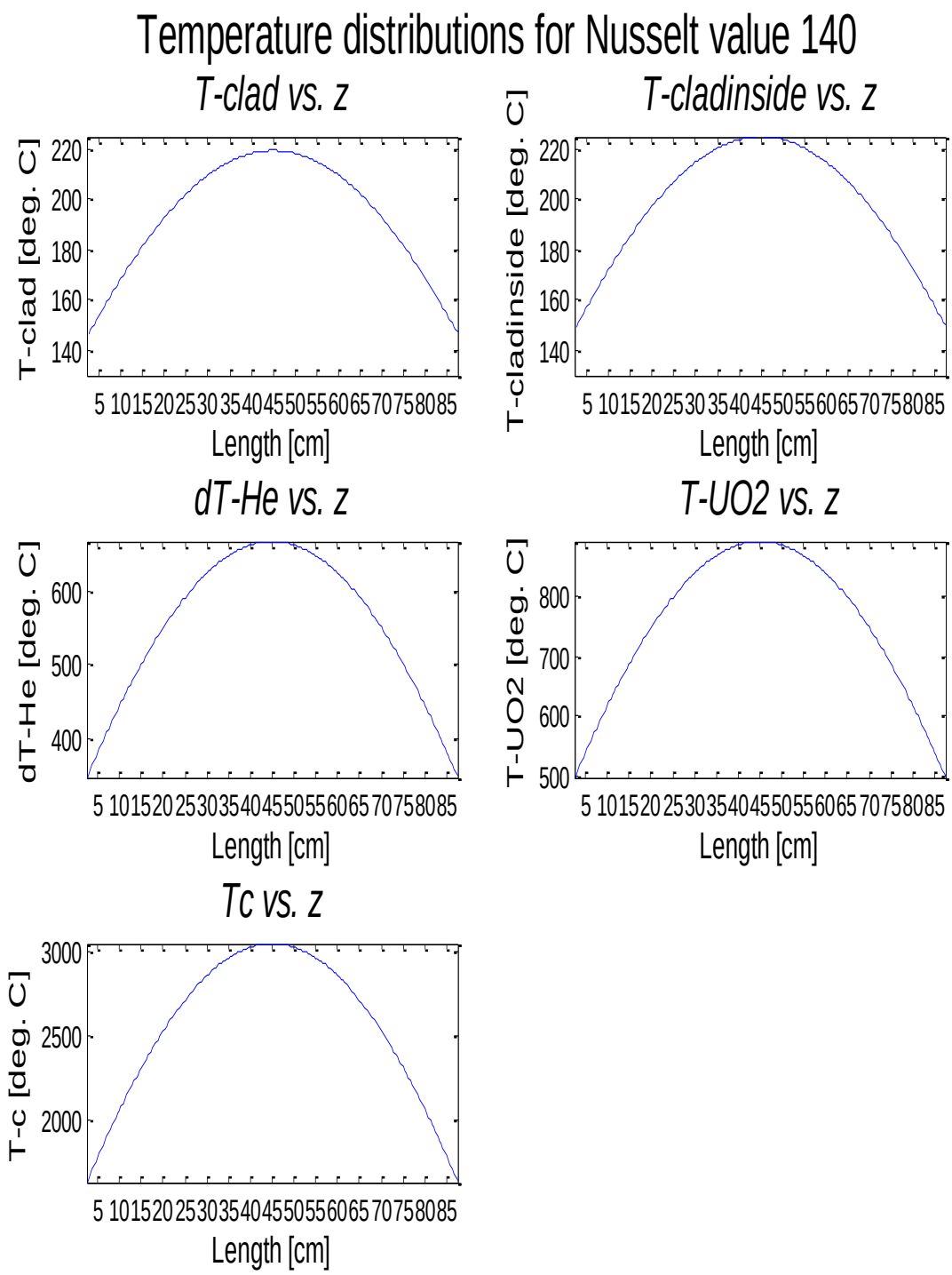

Figure 17. *Subplot containing the temperatures from the clad to the centre line of the fuel pellets along the fuel pin length from the Dittus-Boelter correlation of the 5 MW case.*

The subplot with the heading “T-clad vs. z” of Figure 17 shows the temperature distribution for the surface of the aluminium cladding. Here the maximum temperature is 218 °C, and the edges have the lowest maximum temperature of 148 °C. This is well below the melting point of the aluminium cladding of 660 °C [3]. At the inner surface of the aluminium cladding, the maximum temperature is 225 °C, and the lowest maximum temperature is 150 °C. The temperatures are plotted in the subplot with the heading “T-cladinside vs. z” in Figure 17. This is also a safe temperature with respect to the melting point of aluminium. The temperatures across the 0.2 mm thick helium gap are given in Figure 17 with the “dT-He vs. z” heading. Here the increase has a maximum value of 650 °C, and the lowest maximum temperature increase is 350 °C. The subplot with the “T-UO2 vs. z” in Figure 17 shows the maximum temperature of the surface of the uranium oxide fuel pellets to be 890°C, and the edges of the fuel pellets has the lowest maximum temperature of 500 °C. From the surface to the centre line of the fuel pellets, the temperature increases drastically. This is given in Figure 17 as the subplot with the “Tc vs. z” heading. The centre line temperature is at its highest maximum value at 3 050 °C, and at its lowest maximum temperature at the edges with the value 1 600 °C. The maximum temperature is above the melting point of uranium oxide of 2 850 ±30 °C at normal pressure [40].

Figure 18 presents the temperatures of the fuel pin from the 5 MW model and the six Nusselt numbers. The values of the Nusselt numbers are directly related to the heat transfer coefficient through the hydraulic diameter and the thermal conductivity. In Figure 18, the Nusselt numbers are at the left side of the graph, and the units are dimensionless. The increase in temperature follows the same tendency as the 2 MW case, where the temperature increases drastically through the helium gas, and increasing with an even higher through the uranium oxide fuel pellets.

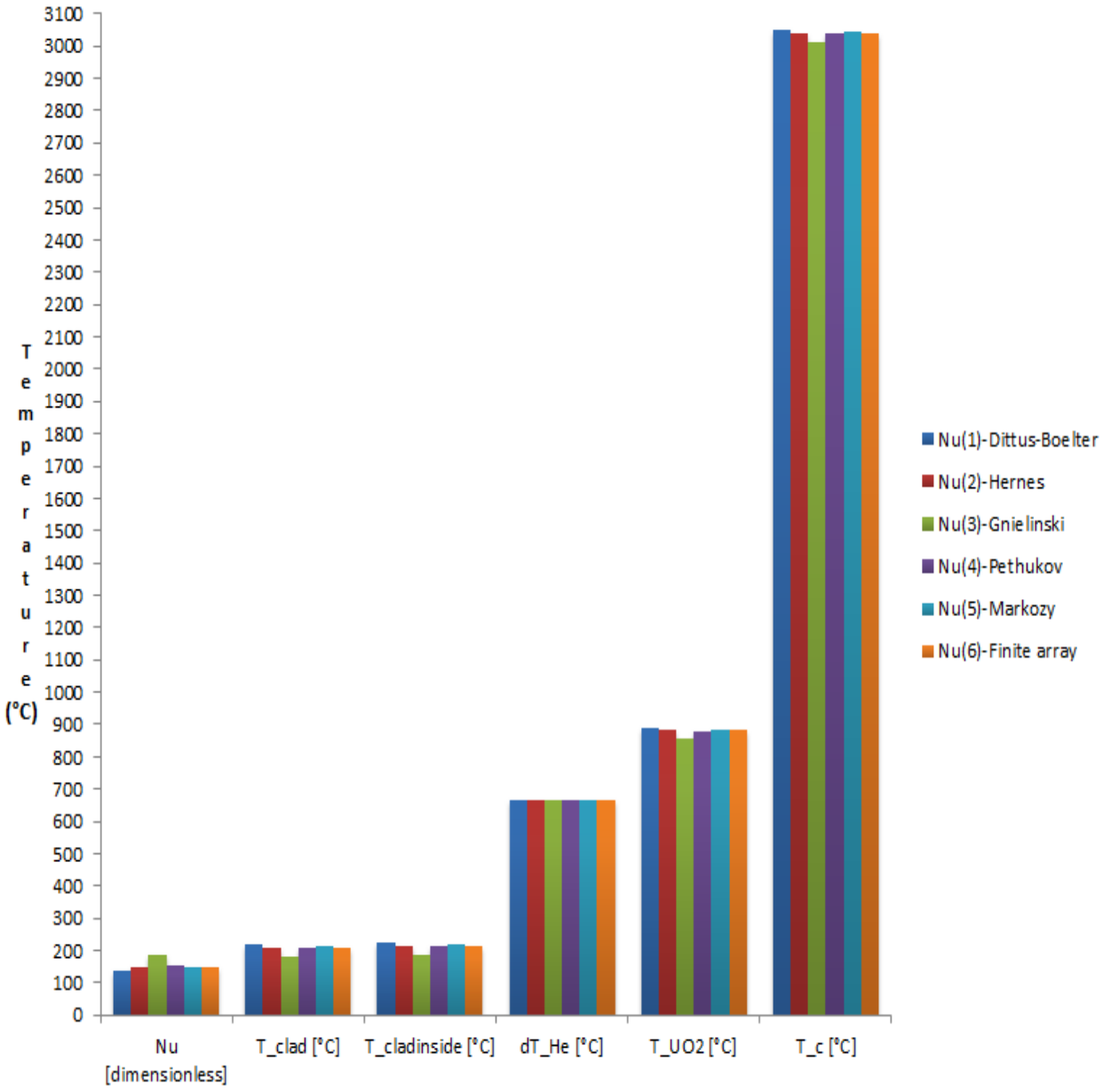

***Figure 18**. Temperatures from the clad to the centre line from the six different Nusselt values from the 5 MW case.*

The increase in power has given high temperatures, especially at the centre line of the fuel pellet, as seen in Figure 18. They are all above 2 865 °C; the melting point of uranium oxide at the present pressure. Another problem that needs to be considered is the temperatures at the cladding. At the 2 MW case the maximum temperature at the cladding of the fuel pin was at 111 °C, and in the 5 MW case the maximum cladding temperatures are all around a hundred

degrees Celsius higher. At these temperatures, the assumption of the heavy water always being at its liquid phase is no longer valid due to nucleate boiling at the surface of the cladding. The boiling point of heavy water at atmospheric pressure (roughly the pressure present in the JEEP II core) is 101.5 °C [41]. The vapour blanket forming at the fuel pin cladding surface deteriorates the heat transfer to such a degree that it is possible that the temperature in the cladding reaches the melting point of aluminium.

Allowing some local boiling at the cladding is accepted to a certain degree, as seen from the nominal operation at JEEP II where the maximum cladding temperature is 111 °C, however; a constant boiling in the core will lead to more tritium being produced as vapour which adds handling risks for the JEEP II personnel, and would thus be unacceptable.

Mitigating measures

Since the temperatures at the centre line of the fuel pellet and at the cladding are unacceptable, attempts to mitigate the high temperatures coming from the power of 5 MW were made in the script. This involved geometrical and flow rate changes. A change in the geometry or the flow rate has a significant effect on the temperatures of the fuel pin. The mitigating measures done in this thesis include:

- Adding extra fuel elements in the core
- Removing the inner shroud of a fuel element
- Reducing the diameter of a fuel pin
- Adding fuel pins in a fuel element
- Increasing the volumetric flow rate

Note that the power is still 5 MW; an addition of fuel pins or fuel elements means that there will be more fuel pins per power. The reduced power per fuel pin will lead to a reduced flux in the core and thus the temperatures are also reduced. All the geometrical alterations results in reduced temperatures. A change in the volumetric flow rate makes the convective heat transfer at the cladding/heavy water junction more effective.

Several different geometrical alterations were examined and implemented in the script, and the alterations that were deemed feasible are presented below. The upgrade to 5 MW only takes the thermal hydraulics and mechanics from the geometrical mitigations into account, even though an upgrade of effect implies an increased enrichment grade and following from this a different situation with respect to activity and neutronics in the core.

GEOMETRICAL MITIGATIONS

ADDING A FUEL PIN IN THE SHROUD

To reduce the temperatures from the 5 MW case, a geometrical mitigation involving the addition of a fuel pin was done in the script. Adding more fuel pins will reduce the amount of heat generated per fuel pin, and a decrease in the overall temperatures will occur. Firstly, the geometrical change leads to a decrease in the pitch, i.e. the distance between two fuel pins. This comes from inserting an extra fuel pin in the shroud, while maintaining the same outer diameter of the pins. The pitch-to-diameter ratio (PDR) decreases, since the diameter is the same and the pitch decreases. Lastly, the chord length between two fuel pins also decreases. The iterating calculation of the pitch and PDR for 11 and 12 pins is given below.

```
c = 15; % [mm] Diameter of fuel pin
r_s = 32; % [mm] Radius of fuel centre circle

for j = 11:12

deg = (2·asind(c/(2·r_s)))
degp2p = (360 – (deg·j))/j
cp2p = 2·r·sind(degp2p/2)
Pitch = (D_o + cp2p)
PDR = (Pitch)/D_o
end
```

The “for”-loop calculates for 11 and 12 fuel pins. At first it calculates the angular degrees per fuel fin with respect to fuel element centre. The c is the

diameter of the fuel pin. The next step is calculating the angular degrees between two fuel pins degp2p, i.e. two adjacent pins from outer diameter to outer diameter. Then the respective chord length of the distance between two fuel pins are calculated, the cp2p. The pitch is then found by adding two radiuses, or a diameter of a fuel pin. The PDR is calculated by dividing the pitch by the diameter of a fuel pin. The iteration can be altered with respect to the number fuel pins, but is in reality only valid for 12 pins or fewer. This is due to the amount of space the pins takes within the shroud. These values are shown in Table 6.

Table 6. *Pitch, the pitch-to-diameter ratio and the distance between two fuel pins for 11 and 12 pins placed within the shroud.*

Fuel pins	Pitch/mm	PDR	R2R/mm
11	18.1	1.2	3.1
12	16.6	1.1	1.6

From the tabulated values of Table 6 it is clear that the more pins that are placed within the shroud, the more confined the situation gets. The distance between the fuel pins (R2R) is lowered to just above 1.6 mm when there are 12 pins within the shroud. And the pitch-to diameter ratio is decreased to 1.1. The change implies a new design for the shroud, making more room for extra pins within the shroud. The original geometry of 11 fuel pins and the geometry of the fuel element when another fuel pin is placed within are illustrated in Figure 19.

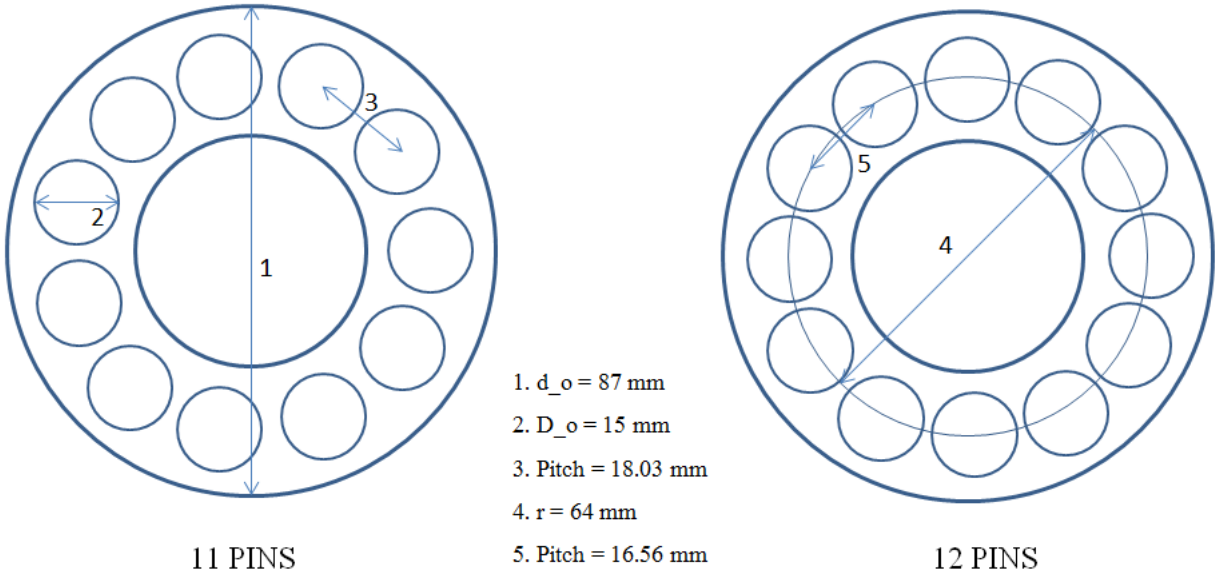

***Figure 19**. Pitch, outer diameter and fuel element diameter for the original geometry of 11 pins, and the pitch and the diameter of the fuel pin centre line for 12 pins.*

From Figure 19 the different geometries of 11 and 12 fuel pins are presented. The shroud containing 12 pins shows a more confined situation. The temperatures from the geometrical mitigation with 12 pins within the shroud are shown in Table 7. The diameters are the same for 11 and 12 fuel pins within the shroud.

***Table 7.** Temperatures of the fuel pin when the shroud has 12 fuel pins placed within.*

	T_clad/°C	T_cladinside/°C	dT_He/°C	T_UO2/°C	T_c /°C
Nu(1)	196	201	611	812	2790
Nu(2)	190	195	611	806	2783
Nu(3)	166	171	611	782	2760
Nu(4)	186	192	611	802	2780
Nu(5)	197	202	611	813	2790
Nu(6)	194	199	611	810	2788

Table 7 shows the temperatures from the 5 MW model when the geometry of the shroud has been changed to contain 12 fuel pins. The maximum heat flux is here at 1.05 MW/m^2, around 590 kW more than the 2 MW case. The maximum heat flux gives a DNBR of 1.4. The value of the flux is lower than the original 5 MW case, the change being due to increasing the total amount of fuel pins from 209 to 228. Adding another fuel pin in the shroud has decreased both the temperature of the centre line and the temperature of the cladding. The centre line of the fuel pellets is now at a maximum average of just below 2 800 °C, and the average of the maximum cladding temperatures is 191 °C. An increase in the heat transferring area has decreased the overall temperature from the original geometry of 11 pins. There is still a high temperature at the surface of the cladding, and the centre line temperature is at a dangerously high level.

Concentric fuel bundles

The second geometrical mitigation measure was to remove the inner shroud, which results in more room for additional fuel pins. The removal of the inner shroud made it possible to add another circular set of fuel pins; the original outer circular fuel bundle of 11 pins was kept, while an inner circular fuel bundle was placed coaxially with the outer. The inner fuel bundle diameter is around half the size of the outer circular fuel bundle. The inner cylindrical fuel bundle has a total of 5 fuel pins on its circumference, resulting in a total of 16 fuel pins within a fuel element. The sketch of a fuel element with 16 fuel pins is presented in Figure 20.

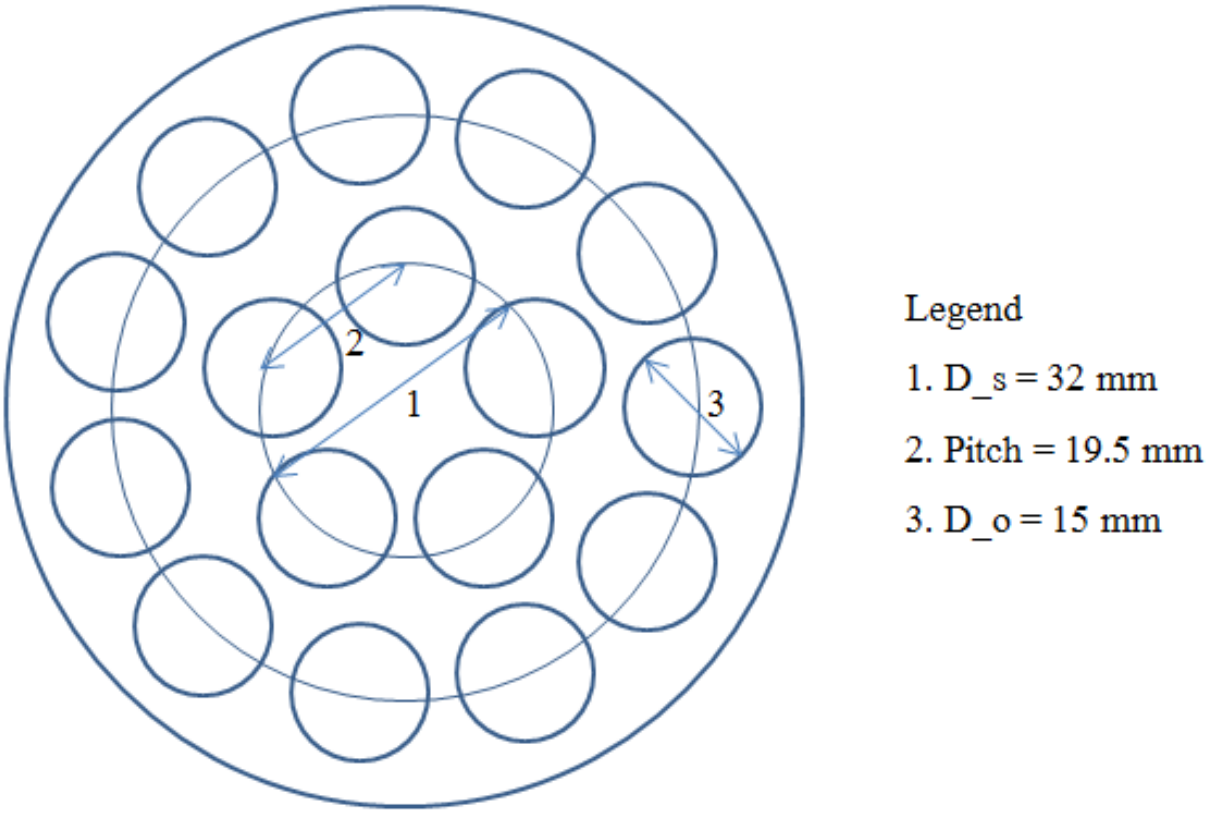

Figure 20. *Cross section of a fuel element with the inner shroud removed and replaced with a circular fuel bundle.*

The pitch of the outer circular fuel bundle is the same; 18.1 mm. The pitch of the inner cylindrical fuel bundle is larger than the outer pitch; 19.5 mm. The PDR is larger for the inner bundle than the outer; 1.3. Due to the neutronics effects at the inner cylindrical fuel bundle, the pitch is set larger. The inner bundle gets neutrons from the outer fuel bundle and the other fuel pins located at the inner fuel bundle which results in an increased neutron economy at the inner fuel bundle with respect to the outer.

The geometry of the shroud is radically changed when adding 5 fuel pins and removing the inner shroud. The area of the fuel bundle is increased by making the whole cross section of the fuel element available for fuel pins. The wetted perimeter also increases, since another 5 fuel pins are included in the fuel element. This will radically change the Reynolds number and subsequently the Nusselt numbers.

The addition of 5 fuel pins in a fuel element reduced the temperatures from the unmitigated 5 MW case. The heat flux per fuel pin is reduced, resulting in lower temperatures over a fuel pin. Temperatures from the geometrical mitigation of a circular fuel bundle insertion are shown in Table 8.

Table 8. Temperatures from the mitigating option of removing the shroud and inserting a circular fuel bundle.

	Nu	T_clad/°C	T_cladinside/°C	dT_He/°C	T_UO2/°C	T_c /°C
Nu(1)	129	186	190	458	648	2132
Nu(2)	137	179	183	458	641	2124
Nu(3)	167	159	163	458	621	2104
Nu(4)	139	177	181	458	639	2123
Nu(5)	136	180	184	458	642	2125
Nu(6)	139	177	181	458	639	2122

The temperatures have been reduced drastically from the unmitigated 5 MW case, as is shown in Table 8. The maximum fuel centre line temperature that previously was above 3 000 °C is now at an average of 2 120 °C. The maximum cladding temperature has not decreased to such a degree as the centre line; the average maximum cladding temperature is 176°C. The DNBR is in this case at 1.9. The addition of an inner circular fuel bundle in a fuel element made a larger impact than the addition of a fuel pin within the shroud.

Reducing the fuel pin diameter

The diameter of the fuel pins can be reduced to make more room for fuel pins within an element. The inner shroud is as in the previous example removed. The diameter was reduced from 15 mm to 10 mm [42]. The size of the helium gap and cladding thickness was kept the same as the 2 MW case; 0.2 mm and 2 mm. The other diameters given, the fuel pellet was adjusted to fit in the fuel pin which gave a diameter of 7.8 mm.

The reduction of the fuel pin diameter made it possible to insert more fuel pins in a fuel element. A total of 25 fuel pins with a diameter of 10 mm were inserted in a fuel element. This is shown in Figure 21. The outer diameter of the element is still the same; 87 mm.

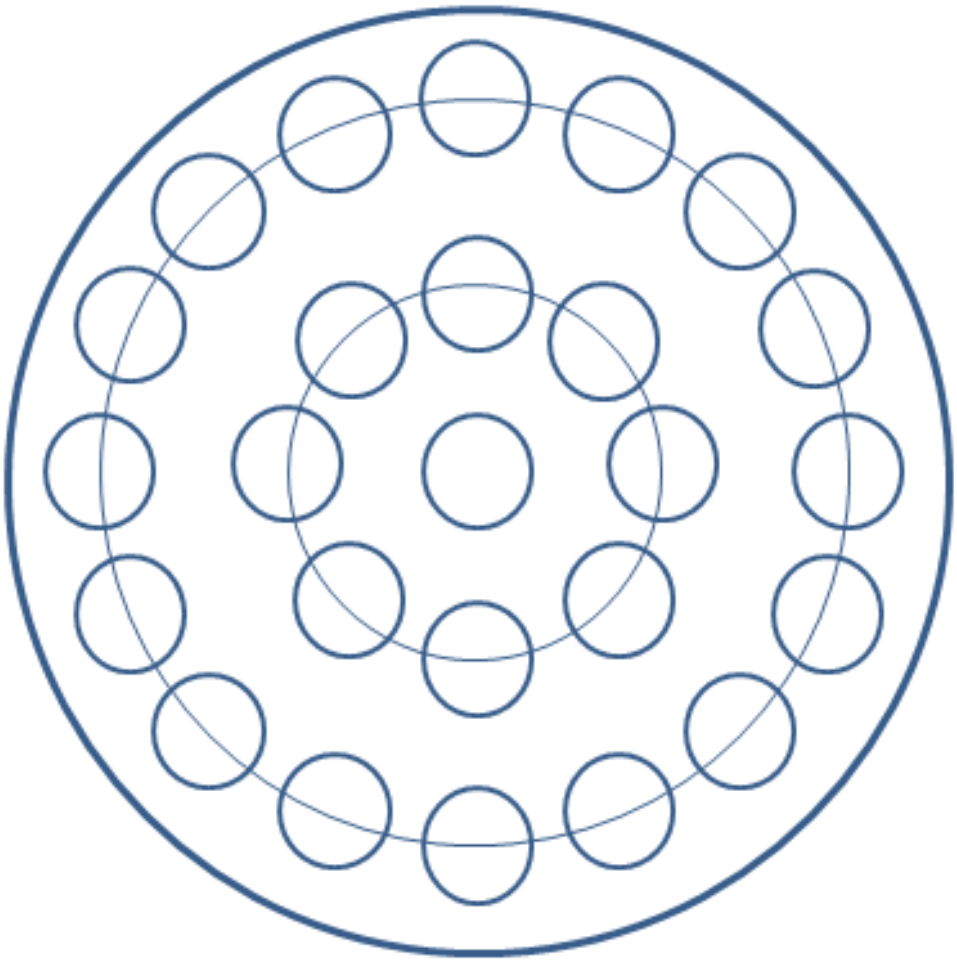

Figure 21. *Cross section of a fuel element when the outer diameter of a fuel pin is reduced to 10 mm. The inner shroud is removed and replaced with a centre fuel pin and a circular fuel bundle.*

The geometry of Figure 21 involves a new pitch and PDR. The pitch of the outer circular fuel bundle is now 13.5 mm, with a PDR of 1.35. The pitch of the inner circular fuel bundle is 13.4, with a PDR of 1.34. There has also been placed a single fuel pin at the centre of the fuel element. The new geometry also involves changing the thermal hydraulic equations in the script. The

resulting temperatures from placing 25 fuel pins with an outer diameter of 10 mm within the shroud are shown in Table 9.

Table 9. Temperatures from the mitigating option of reducing the outer diameter of a fuel pin and adding a circular fuel bundle and a centre fuel pin.

	Nu	T_clad/°C	T_cladinside/°C	dT_He/°C	T_UO2/°C	T_c /°C
Nu(1)	126	212	216	478	694	1643
Nu(2)	135	202	206	478	684	1633
Nu(3)	162	179	183	478	661	1610
Nu(4)	136	202	205	478	683	1632
Nu(5)	163	179	183	478	660	1610
Nu(6)	168	176	179	478	657	1606

The results from the mitigating measure of fuel pin diameter reduction shows that the average maximum cladding temperature is slightly higher than the unmitigated temperatures, and that the average maximum centre line temperatures are ca. 1 400 ˚C lower than the unmitigated temperatures of just above 3 000 ˚C. The DNBR is in this case ca. 2.

Increasing the volumetric flow rate

The volumetric flow rate from the operation of the reactor is 235 m^3/h, whereas the new flow rate is taken from the internal report from IFE regarding a possible upgrade of the reactor [1]. The flow rates of the report covering the upgrade were 235 m^3/h, 300 m^3/h and 350 m^3/h. The highest flow rate, and thus the flow rate affecting the temperatures the most due to increased convection, is 350 m^3/h [1]. The temperatures coming from the change in the volumetric flow rate is presented are Table 10.

Table 10. Temperatures from the mitigating option of increasing the volumetric flow rate to 350 m³/h.

	Nu	T_clad/°C	T_cladinside/°C	dT_He/°C	T_UO2/°C	T_c
Nu(1)	200	169	174	666	841	2998
Nu(2)	211	163	168	666	835	2992
Nu(3)	273	140	146	666	812	2970
Nu(4)	220	159	164	666	831	2988
Nu(5)	208	164	170	666	836	2994
Nu(6)	214	162	167	666	834	2991

The change of the volumetric flow rate increased the Nusselt number to a large degree, as shown in Table 10. The Reynolds number increases because the velocity of the water flowing through the fuel element increases. The Nusselt numbers changes due to its dependency on the Reynolds number.

The average maximum temperature at the cladding is 159 °C, a much lower temperature than the unmitigated case and the geometrical mitigation cases. The maximum average temperature for the centre line of the fuel pellets is 2 989 °C, a slightly lower temperature than the unmitigated case and a higher temperature than the geometrical mitigation cases. The centre line temperature is this high because the large flow rate is most effective at the cladding surface, reducing the temperature of the cladding. There is still the large heat flux of approximately 1 MW/m^2 that needs to be transferred from the centre line and out. Increasing the volumetric flow rate results in a DNBR of 1.5.

Adding fuel elements in the core

The geometrical mitigations all reduced the temperatures of the fuel pin. The higher flow rate was most effective for the cladding temperatures, whereas the geometrical mitigations were most effective for the fuel centre line temperatures. There are unique difficulties included in the realization of each of the measures. To get an even greater reduction in the temperatures, the two most effective geometrical measures of reducing the fuel pin diameter and

inserting a circular fuel bundle were calculated in the script with a changing amount of fuel elements and a changing flow rate.

The core of the JEEP II is designed to contain 45 fuel elements. This means that a total of 45-19 = 26 additional fuel elements can be included in the script to reduce the temperatures further. A total of 26 calculations with 20 to 45 fuel elements were taken in the script for the unmitigated (nominal) case, reduced diameter case and circular fuel bundles case to investigate the effects of an addition of fuel elements in the core. The volumetric flow rate was here increased so as to keep the velocity through an element constant at 1.3 m/s while increasing the total amount of fuel elements in the core. The result is shown in Figure 22.

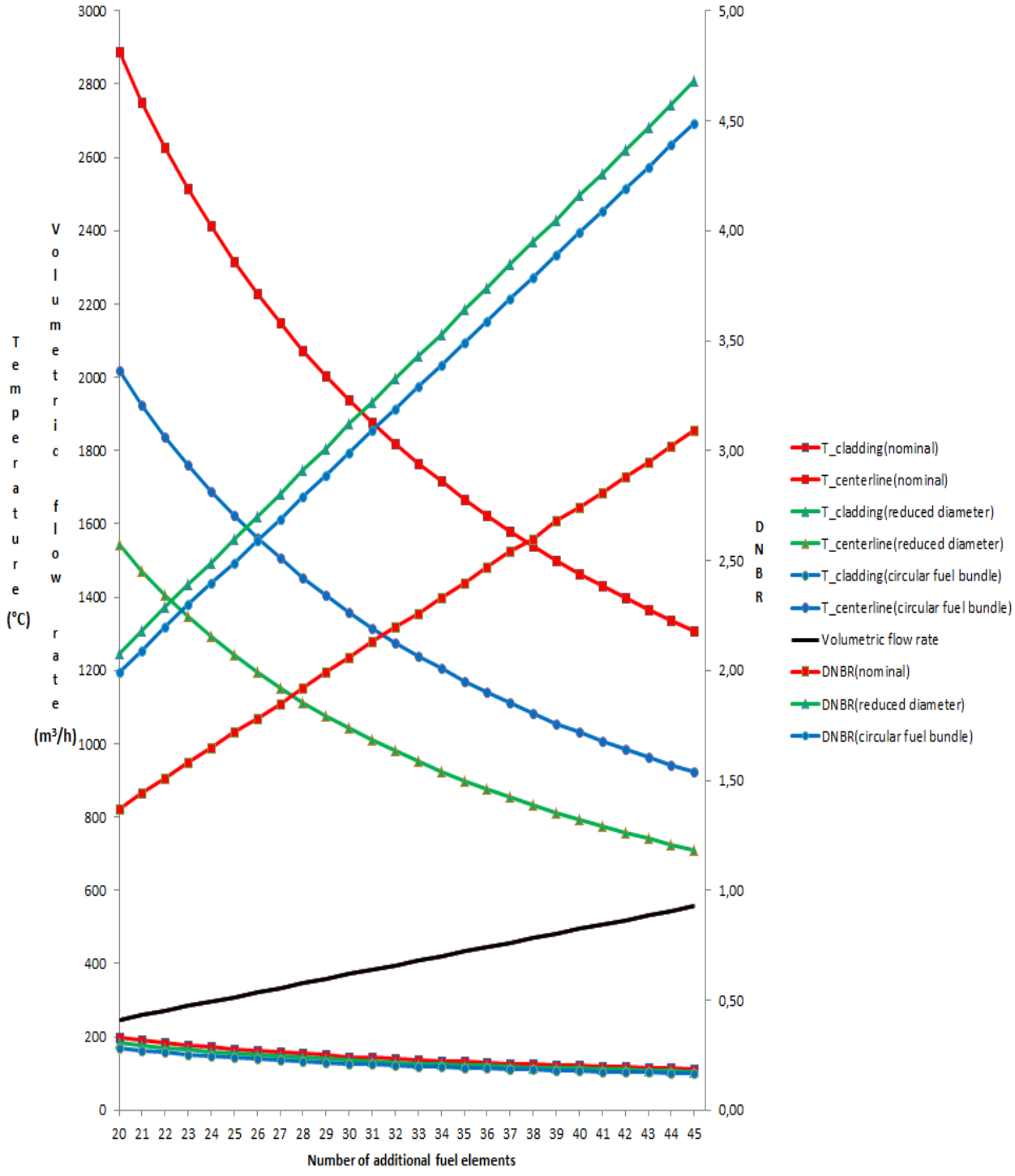

***Figure 22**. Cladding temperature, the fuel centre line temperature and the DNBR for the unmitigated (nominal) case, the circular fuel bundle case and the reduced fuel pin diameter case for 20 to 45 fuel elements in the core. The volumetric flow rate is increased proportionally with added fuel elements such that the velocity through a fuel element remains constant.*

From Figure 22 the effect of additional fuel elements is visualized clearly. The fuel centre line temperature for the nominal case has a reduction in temperatures when the amount of fuel elements in the core is increased from 20 to 45; 1 500 °C. The DNBR for these cases increases from 1.4 to 3.1. The reduced diameter case has a reduction in fuel centre line temperature of 710 °C, and an increase in the DNBR from 2.1 to 4.7. The circular fuel bundles case has a reduction in fuel centre line temperature of 1 100 °C, and an increase in the DNBR from 2 to 4.5. The change in cladding temperatures is 86 °C for the nominal case, 78 °C for the reduced fuel pin diameter case and 68 °C for the circular fuel bundles case. When the velocity of the heavy water through a fuel element was kept constant while increasing the total amount of fuel elements an increase in the volumetric flow rate from 250 m^3/h to 560 m^3/h was present.

The average maximum fuel centre line temperature for the unmitigated case with a total of 45 fuel elements is 1 308 °C and the average maximum cladding temperature is 113 °C. For the reduction in fuel pin diameter case the average maximum fuel centre line temperature is 710 °C and the average maximum cladding temperature is 106 °C. For the addition of a circular fuel bundle the average maximum fuel centre line temperature is 922 °C and the average maximum cladding temperature is 101 °C. It is clear that the increased volumetric flow rate is most effective in reducing the cladding temperatures, and the reduced fuel pin diameter case is most effective for reducing the fuel centre line temperature.

6. Discussion

The 2 MW model

Finding the right method to perform thermal hydraulic calculations on the JEEP II without empirical research is not an exact science. Six Nusselt correlations, all designed for various flow regimes and flow geometries, were chosen to investigate the applicability on the JEEP II geometry. From the Nusselt numbers the heat transfer coefficients are calculated. The heat transfer coefficients and the Nusselt numbers are presented in Table 3. The average of the heat transfer coefficients was consistent with the calculated value from the Safety report, which supported the further temperature calculations.

The consistency check of the Safety report temperatures with the temperatures from the 2 MW model were done so as to verify the validity of the model. This is in reality the cheapest way to check if the modelling is done in a proper way. Table 4 shows that the script temperatures fit accurately with the empirical values from the reactor operation. The temperature deviations shown in Table 4 are deemed to be not too large, and the 2 MW model was approved on the basis of this.

The 5 MW model

The extrapolation from the 2 MW model meant that the heat flux and the temperatures in the reactor would increase. The high temperatures from the conservative approach were necessary to verify the validity of the model. The temperatures from the extrapolation were unacceptable; an average maximum centre line temperature of 3 030 °C which is ca. 150 °C above the melting point and an average maximum cladding temperature of 207 °C which involves risks in terms of boiling at the cladding surface and an unacceptable departure from nucleate boiling ratio due to the high safety standards in place at IFE-Kjeller. Based on these results, the 5 MW upgrade of the JEEP II using the

present-day flow rate and fuel element design and layout is deemed unfeasible.

Implications from the upgrade

Increasing the power to 5 MW leads to alterations in how the fuel is designed. As previously mentioned, it is assumed that the 2 MW reactor geometry, i.e. the 19 fuel elements with the 209 fuel pins, can produce 5 MW. This implies a new enrichment grade that can provide 5 MW for a sustained, acceptable period of time.

The higher power level will result in more fission reactions taking place in the core. Associated with this a higher neutron flux and thermal flux will be present in the core, and also more fission products. To maintain the same fuel replacement strategy as is practiced today, a fuel at a higher enrichment would be practical. The increased flux of neutrons will affect the activity in the core, the moderator, the reflector and of course the heat generation.

Safety and risks

The fuel centre line temperature from the 5 MW case will lead to a melting of the fuel, as the melting point of uranium dioxide at the present pressure is 2 865 °C. The cladding temperature will lead to more boiling at the junction between the heavy water and the cladding, and the possibility of departure from nucleate boiling is severely increased. The assumption of the water always being at its liquid phase is then no longer applicable due to the increased boiling. Where the 2 MW operation of the reactor allows some local boiling, the temperatures of the upgrade will lead to permanent boiling.

A 5 MW reactor has higher fuel loading than a 2 MW reactor, and this leads to an ability to sustain a higher neutron flux for a longer period. The high neutron flux will contribute to a greater production of tritium; a toxic substance. Tritium is formed when the deuterium atoms of heavy water absorbs thermal neutrons [43]. Even though the absorption cross section of

this nuclear reaction is small, tritium gas is still produced. If an accident situation is to occur, tritium can pose a danger if it is inhaled. It can also combine with oxygen to form tritiated water molecules which can be absorbed through the skin [43].

Mitigation

Increased flow rate

From the internal IFE report [1] the flow rates were set at 235 m^3/h, 300 m^3/h and 350 m^3/h. The report discussed a power upgrade of 4 MW, but the example of the increased flow rate is still applicable for the 5 MW upgrade. To reduce the temperatures further, the velocity through an element was kept constant while the amount of fuel elements was changed to the maximum value of 45. This gave a flow rate of 560 m^3/h.

A higher flow rate of heavy water leads to more effective heat transfer from the fuel pins to the water. The implications on the circuit system from increasing the flow rate are uncertain, but they will almost certainly have a negative impact [44]. A larger flow rate will put more pressure on the circuit system, and the pipes will need to withstand more friction. The flow channel in the fuel element and the pipes in the circuit are designed for a flow rate of 235 m^3/h, and the increased flow will possibly be too high a flow rate. Thus a new circuit system with more resilient pipes will possibly need to be installed.

Geometrical alterations

Adding a fuel pin in the shroud

The addition of a fuel pin in the shroud is the least dramatic change in geometry. Having 12 fuel pins within the shroud reduces the pitch, the pitch-

to-diameter ratio and the pitch between the outer diameters of two pins. Enough water surrounding the pins are of importance since it both absorbs and carries away the generated heat from fission and moderates the neutrons down to a thermal energy. When the power increases, the pitch should preferably be larger than the lower power case, and in any case not smaller, which is the case when an extra fuel pin is added in the shroud.

The temperatures from the addition of a fuel pin are not severely reduced with respect to the unmitigated case. The average maximum cladding temperature is at 190 °C, and the average maximum centre line temperature is 2 780 °C. The cladding temperature is higher than the temperature from the Safety report, and the centre line temperature is just below the melting point. This geometrical alteration gave the highest centre line temperature of all the mitigating measures, and is therefore not an adequate mitigating measure.

Concentric fuel bundles

This mitigating measure involved removing the inner shroud to make room for additional fuel pins. The diameter of 15 mm was kept, and the pitch from the 2 MW case was kept for the outer circular fuel bundle and increased for the inner circular fuel bundle. The average maximum cladding temperature for this mitigating measure was 176 °C, and the average maximum centre line temperature was 2 122 °C. The temperatures of the centre line are within an acceptable range from the melting point, but the cladding temperatures are much larger than the 2 MW temperatures.

Reducing the pin diameter

The reduction of the original diameter of 15 mm to 10 mm was done to be able to fit more fuel pins within a fuel element. The inner shroud was also removed in this case. A total of 25 fuel elements were placed in a fuel element; an outer circular fuel bundle, an inner circular fuel bundle and a centre fuel pin. The

pitch is larger for the reduced diameter mitigation measure than the 2 MW case, but it now gets smaller inward to the centre. This is not preferred since enough water should flow over the pin to remove the generated heat. A possible solution is to remove a fuel pin from the inner circular fuel bundle to increase the pitch. The average maximum cladding temperature from the geometrical mitigation measure of pin diameter reduction is 192 °C, and the average maximum centre line temperature is 1 622°C.

Adding fuel elements

The addition of a fuel element in the core will eliminate an available spot for inter alia irradiation facilities; however, the core is designed for a total of 45 fuel elements. The result of including an extra fuel element is more fuel pins in total, and a reduced power per fuel pin. This is the same effect as adding more fuel pins in a fuel element, but it is not at the expense of room within the fuel element. Extra fuel elements were added in all the mitigating measures to reduce the associated temperatures from the 5 MW further. The problems from the other mitigating options are inherent when extra fuel elements are added in the core.

Exploiting the core design of the JEEP II, the addition of fuel elements up to a total of 45 gave promising temperatures. The volumetric flow rate is increased linearly with the amount of fuel elements so as to keep the velocity through a fuel element constant. The maximum average fuel centre line temperature that was most promising was from the reduced diameter option; 710 °C. The maximum average cladding temperature that was most promising was from the circular fuel bundles option; 145 °C. The high cladding temperatures from all the mitigating options can be reduced by increasing the volumetric flow rate. A total of 45 fuel elements are justifiable from a thermal hydraulic point of view, but it is debatable whether this amount of fuel elements is feasible with respect to research facilities and operation of the reactor. From a thermal hydraulic viewpoint the addition of fuel elements is deemed as a good solution.

Error analysis

There are uncertainties involved in finding the temperatures of the fuel pin. Firstly, there are uncertainties in the thermo physical properties of the heavy water as these are identified using interpolation between tabulated values. The Reynolds number and the Prandtl number are calculated using these properties, thus the uncertainty propagates to the Nusselt number.

In this thesis, six different flow correlations are used to find the Nusselt numbers. Each of these correlations has their own uncertainty with respect to the fuel element geometry and coolant flow in the reactor. The heat transfer coefficient is calculated via the Nusselt number.

The temperatures of the individual fuel pins are calculated from the heat transfer coefficients, each coming from one of the six Nusselt correlations. The average maximum temperatures are identified from the pin temperatures, and then compared with the empirical values from the operation of the JEEP II to validate the model assumptions.

The results of the validation process above justify the extrapolation from 2 to 5 MW. The 5 MW model has inherently similar uncertainties built into the model as the 2 MW design, however, the iteration process to identify the outlet temperature, assuming a certain temperature for the bulk heavy water, introduces additional uncertainty.

However, as the considerations above are primarily completed to verify the validity of the model, and the empirical values from the reactor operation is applied, there is no need for further evaluation of the uncertainties with respect to the results of the work.

7. Conclusion

The different flow correlations chosen for the JEEP II geometry gave acceptable temperatures with respect to the empirical values from the operation of the JEEP II. This made it possible to verify the validity if the 2 MW model, and the extrapolation to 5 MW was thus carried out, resulting in unacceptable temperatures in the centre line of the fuel pellets and the cladding of the fuel pins. The average maximum centre line temperature of above 3 000 °C would have resulted in a melting of the fuel and the higher maximum heat flux would have severely increased the possibility of departure from nucleate boiling at the cladding.

Due to the unacceptable temperatures from the extrapolation, mitigating measures were implemented in the script. The geometrical measure taken to reduce the associated temperatures from the upgrade that was considered not feasible was the addition of a fuel pin with the shroud. The geometrical mitigating measures of reducing the fuel pin diameter, inserting a circular fuel bundle and adding fuel elements gave promising temperatures, and the combination of the geometrical measures with the increased volumetric flow rate led to temperatures equal to or lower than the 2 MW case . The mitigated 5 MW model with 45 fuel elements, one of the two most promising fuel pin alterations and a flow rate of 560 m^3/h is from a thermal hydraulic viewpoint deemed as a feasible model.

The research question can thus be confirmed; the temperatures and the heat flux in the fuel pins of the reactor can be kept at 2 MW levels or lower after a power upgrade from 2 to 5 MW.

8. BIBLIOGRAPHY

[1] E. Andersen, U. Been, T. Riste and H. Sekkesæter, "Upgrading the JEEP II Reactor," IFE, Kjeller, 1988.

[2] K. Bendiksen, Interviewee, [Interview]. 23 November 2012.

[3] H. Sekkesæter, "Melting of Core at a LOCA," IFE, Kjeller, 1966.

[4] A. Lundberg, "JEEP II, Burnout calculations," IFE, Kjeller, 1965.

[5] H. E. Andås and T. Ustaheim, "Kjøleforløpet ved stopp av vannsirkulasjonen i hovedkjølekretsen," IFE, Kjeller, 1965.

[6] T. Hernes, "Brenselselement JEEP II - Konstruksjons- og prøverapport," IFE, Kjeller, 1963.

[7] S. Mullet, "JEEP II Shutdown with Forced Loss of Cooling," IFE, Kjeller, 2011.

[8] J. Ahlf and J. Schinkel, "Upgrading and modernization of the High Flux Reactor Petten," *Nuclear Engineering and Design,* vol. 137, pp. 49-56, 1992.

[9] H. Khater, T. Abu-EL-Maty and S. E.-D. EL-Morshdy, "Thermal hydraulic modeling of reactivity accident in MTR reactors," Annals of Nuclear Energy, 2007.

[10] O. Njølstad, Strålende forskning, Oslo: Tano Aschehoug, 1999.

[11] E. Andersen, K. Caspersen, H. S. Olsen, T. Skardhamar, A. T. Skjeltorp and O. Steinsvoll, Oppgradering av JEEP II, Kjeller: IFE, 1996.

[12] G. H. e. a. Lander, "Scientific Prospects for Neutron Scattering with Present and Future Sources," Autrans, 1996.

[13] "http://www.world-nuclear.org/info/inf01.html," World Nuclear Association. [Online]. [Accessed 27 11 2012].

[14] "http://www.world-nuclear.org/info/inf32.html," World Nuclear Association. [Online]. [Accessed 27 11 2012].

[15] E. S. Beckjord and e. al., "The Future of Nuclear Power," Massachusets Institute of Technology, Cambridge, 2003.

[16] "http://www.world-nuclear.org/uploadedImages/org/info/gross_and_net_power.png," World Nuclear. [Online]. [Accessed 25 11 2012].

[17] "http://www.world-nuclear.org/info/inf61.html," World Nuclear Association. [Online]. [Accessed 27 11 2012].

[18] "http://www.emtr.eu/_img/hfr/HFR1.jpg," European Materials Testing Reactors, [Online]. Available: http://www.emtr.eu/_img/hfr/HFR1.jpg. [Accessed 2 12 2012].

[19] J. M. Siracusa, Nuclear weapons: A very short introduction, New York: Oxford University Press Inc.

, 2008.

[20] J. S. Lilley, Nuclear Physics - Principles and Applications, Chichester: John Wiley & Sons, Ltd. , 2001.

[21] "http://imagine.gsfc.nasa.gov/Images/teachers/posters/elements/booklet/energy_big.jpg," NASA. [Online]. [Accessed 27 11 2012].

[22] "http://t2.lanl.gov/tour/u235nf.gif," Los Alomos National Laboratory. [Online]. [Accessed 3 12 2012].

[23] P. D. Macián-Juan, "Grundlagen der Nukleartechnik," Technische Universität München, Munic, 2011.

[24] "http://world-nuclear.org/how/enrichment.html," World Nuclear Association. [Online]. [Accessed 28 11 2012].

[25] "http://nuclearpoweryesplease.org/blog/wp-content/uploads/u235nf.gif," [Online]. [Accessed 20 11 2012].

[26] D. P. DeWitt and F. P. Incropera, Fundamentals of Heat and Mass Transfer, vol. V, Hoboken: John Wiley & Sons, 2001.

[27] K. D. Kok, Nuclear Engineering Handbook, CRC Press, 2009.

[28] Y. A. Cengel, Heat and Mass Transfer: A Practical Approach (SI Units), vol. III, New York: McGraw-Hill, 2006.

[29] N. E. Todreas and S. M. Kazimi, Nuclear Systems I, New York: Hemisphere Publishing Corporation, 1989.

[30] S. Kakac, R. K. Shah and W. Aung, Handbook of single-phase convective heat transfer, New York: John Wiley & Sons, Inc., 1987.

[31] J. Bukovsky and K. Haack, Heavy Water Handbook, Roskilde: Risø National Laboratory, 1994.

[32] S. Mullet, Interviewee, [Interview]. 16 11 2012.

[33] IFE, “JEEP II - Security Report, Part I - Reactor Operation,” IFE, Kjeller, 2011.

[34] S. Mullet, "HELIOS-code of JEEP II reactor (E-mail, 7.12.12)," IFE, Kjeller, 2012.

[35] Mathworks, "www.mathworks.se/help/matlab/ref/interp1.html," [Online]. [Accessed 4 11 2012].

[36] I. R. IFE, "Axial Flux Shape," IFE, Kjeller, 2010.

[37] “http://www.mathworks.se/help/matlab/ref/for.html,” Mathworks. [Online]. [Accessed 3 11 2012].

[38] Mathworks, "mathworks.se/help/matlab/matlab_prog/operators.html," [Online]. [Accessed 2 11 2012].

[39] J. R. Taylor, An Introduction to Error Analysis, Sausalito: University Science Books, 1997.

[40] S. G. Popov, J. J. Carbajo, V. K. Ivanov and G. L. Yoder, "Thermophysical Properties of MOX and UO2 Fuels Including the Effects of Irradiation," Oak Ridge National Laboratory, Tennessee, 2000.

[41] "http://www.lsbu.ac.uk/water/data.html," London South Bank University. [Online]. [Accessed 2 1 2013].

[42] Holte, Interviewee, [Interview]. 30 11 2012.

[43] “http://en.wikipedia.org/wiki/Tritium,” Wikipedia. [Online]. [Accessed 2 12 2012].

[44] S. Hval, Interviewee, [Interview]. 29 8 2012.

[45] A. Axmann, K. Böning and M. Rottmann, "FRM-II - The new German research reactor," *Nuclear Engineering and Design,* vol. 178, no. 1, pp. 127-133, 1997.

9. List of figures

10. List of tables

11. APPENDIX

A1 MODELLING THE 2 MW REACTOR

```
% ~~~~~~~~~~~~~~~~~~~~~~~~~~~~~~~~~~~~~~~~~~~~~~~~~~~~~~~~~~~~~~~~~~~~~~~~~~~~
%   Modelling the 2 MW Research reactor JEEP II
%   By Erik Henriksen
% ~~~~~~~~~~~~~~~~~~~~~~~~~~~~~~~~~~~~~~~~~~~~~~~~~~~~~~~~~~~~~~~~~~~~~~~~~~~~

%    Assumptions taken
% 1. Continuous velocity distribution within shroud
% 2. The heavy water is always at its liquid phase
% 3. The shroud surfaces are smooth
% 4. A fully developed flow
% 5. Heat flux over element length follows a cosine distribution, implying a
cosine neutron flux distribution (NSI p. 315)
% 6. No heat transport in axial direction, fuel pin/diameter >10 neglect the
axial heat transfer within the fuel relative to the radial (NSI p.316)
% 7. Average thermal conductivities
% 8. Inlet water temperature t_in = 50 degrees Celsius
% 9. Outlet water temperature t_out = 56 degrees Celsius
% 10. All control rods out of the core, and a hot spot factor of 2.04
% 11. The fuel is unirradiated


clear all

N = 19;              % Number of fuel elements
n = 11;              % Number of fuel pins per element
d_f = 12.8*10^-3;    % [m] Diameter of fuel pellet
D_o = 0.015;         % [m] outer diameter of pin
D_i = 0.013;         % [m] inner diameter of pin cladding
d_o=0.087;           % [m] outer diameter of fuel element
d_i=0.041;           % [m] inner diameter of fuel element
d_m = 0.01295;       % [m] Mean diameter of He-layer
z_vector = (-pi*0.325):0.01:(pi*0.325);   % [m] Active length of fuel pin,
string
z_scalar = 0.9;           % [m] Active length of fuel pin, scalar


% Properties of heavy water (D2O) at 56 degrees C. and 1 atm

x= 56; % Temperature of heavy water

t_rho = 50:2:70;
c1 = [1095.650 1094.691 1093.733 1092.657 1091.703...
1090.513 1089.443 1088.258 1087.075 1085.894 1084.716];
rho=interp1(t_rho,c1,x); % Interpolating for density of heavy water at x
degrees

t_mu = 50:10:70;
```

```
c2 = [651.2*10^-6 551.8*10^-6 475.7*10^-6];
mu=interp1(t_mu,c2,x); % Interpolating for dynamic viscosity of heavy water
at x degrees

t_cp = 50:5:70;
c3 = [4197.3 4196.4 4196.1 4196.5 4197.5];
c_p=interp1(t_cp,c3,x); % Interpolating for specific heat capacity of heavy
water at x degrees

t_k = 50:10:70;
c4 = [0.618 0.625 0.629];
k=interp1(t_k,c4,x); % Interpolating for thermal conductivity of heavy water
at x degrees

Pr=(c_p*mu/k); % Prandtl number
Q = 2*10^6; % [W] Power level of reactor
G = 235/3600; % [m^3/s] Volumetric flow rate
Pf = 2.04; % Hot spot factor

q_av = Q.*cos(z_vector)/(z_scalar*N*n*pi*D_o) % [W/m^2] Average heat flux
from a fuel pin
q_max = Pf*q_av % [W/m^2] Maximum heat flux from a fuel pin
figure('name','Maximum heat flux')
plot(q_max)
axis tight
set(gca,'xtick',7:12:200,'xTickLabel',{'5', '10', '15',
'20','25','30','35',...
'40','45','50','55','60','65','70','75','80','85'})
ylabel('W/m^2 [C]','FontSize',12);
xlabel('Length [cm]','FontSize',12);
title('\it{Maximum heat flux}','FontSize',16);
T_out = 56; % [C]
T_in = 50; % [C]

A =(pi/4)*((d_o)^2-(d_i)^2)-(n*pi/4*D_o^2); % [m^2] Area of fuel bundle, one
element
Wd = (pi*d_o+pi*d_i+n*pi*D_o); % [m] Wetted diameter of flow
D_h = 4*A/Wd; % [m] Hydraulic diameter
v = (G/N)/A; % [m/s] Velocity through one fuel element
Re = rho*v*D_h/mu; % Reynolds number


% Nusselt number and h calculations

Nu(1) = 0.023*(Re^0.8)*(Pr^0.4) % Dittus-Boelter
Nu(2) = 0.032*(Re^0.8)*(Pr^0.37)*(D_h/z_scalar)^(0.054) % Nusselt number,
from Hernes - safety report
f = ((0.790*log(Re))-1.64)^-2; % Friction factor for smooth tubes from
Pethukov, Incropera p. 490  Closest to the correlations without friction
factor, chosen for this reason
Nu(3) = ((f/8)*(Re-1000)*Pr)/(1+((12.7*(f/8)^0.5)*(Pr^0.66)-1)) % Gnielinski
p. 515 Incropera
CO = 1.07 + (900/Re) - (0.63/(1+10*Pr));
Nu(4) = ((f/8)*Re*Pr)/(CO + (12.7*(f/8)^0.5)*((Pr^0.66)-1)) % Petukhov Table
4.4 Kakac
```

```
B = (D_h/D_o);
C = 1+(0.912*(Re^-0.1)*(Pr^0.4)*(1-2.0043*exp(-B))); % C is equal to phi in
formula
Nu(5) = C*(0.023*(Re^0.8)*(Pr^0.4)) % Markozy p. 446 Nuclear Systems I,
Finite array "Nu is insensitive to the boundary conditions for Pr>0.7", Nu
are accurate to within 10 % when P/D > 1.12
A = 0.144*Re^0.25;
Nu(6) = (1+(A/(z_scalar/D_h)))*(C*(0.023*(Re^0.8)*(Pr^0.4))) % Entrance
region effect, p.448 NSI, tubes with bell mouth. For L/D_h > 0.693Re^0.25
h = k.*Nu/D_h % [W/m^2*K] heat transfer coefficient

TNu = [Nu(1) Nu(2) Nu(3) Nu(4) Nu(5) Nu(6)];
xlswrite('Nusselt number',TNu) % Tabulating the Nusselt numbers

Th = [h(1)' h(2)' h(3)' h(4)' h(5)' h(6)'];
xlswrite('Heat transfer coefficient',Th) % Tabulating the heat transfer
coefficients

% Iterating for the six different correlations

s = 1;
for s = 1:6
    b = [h(1) h(2) h(3) h(4) h(5) h(6)];

T_clad = (q_max/b(s))+T_out  % Finding the temperature of the cladding
T_cladreportmean = 78;   % Average cladding temperature from Safety report
T_cladreportmax = 111    % Maximum cladding temperature from Safety report

% plot(L,T_clad,'-',L,T_cladreportmax,'*');
% axis auto
% legend ('T-clad','T-cladreportmax',5);
% grid on;
% ylabel('Tclad [C]','FontSize',12);
% xlabel('Length [m]','FontSize',12);
% title('\it{Tclad vs. z}','FontSize',16);
% figure

k_al = 221; % [W/m*K] At 100 degrees Celsius, conductivity coefficient, from
Hernes. Could possibly be higher, due to maximum heat flux (k at 120
degrees?)


% Temperature inside of the cladding
T_cladinside = T_clad +
(log(D_o/D_i)*Q*Pf.*cos(z_vector))/(N*n*2*pi*z_scalar*k_al) % [C] Resistance
equation, solved for temperature. Page 151 Yunus


% plot(L,T_cladinside);
% legend ('T-cladinside',2);
% grid on;
% axis auto
% ylabel('Tcladinside [C]','FontSize',12);
% xlabel('Length [m]','FontSize',12);
% title('\it{Tcladinside vs. z}','FontSize',16);
```

```
% figure

h_He = 2000; % [W/m^2*K] Heat transfer coefficient of He-layer, from Hernes
dT_He = ((Q*Pf).*cos(z_vector))/(N*z_scalar*n*pi*d_m*h_He) % [C] Temperature
rise through He-layer, from Hernes
dT_Hemean = 130; % Average increase in temperature over He-gap from Safety
report
dT_Hemax = 266; % Maximum increase in temperature over He-gap from Safety
report

% plot(L,dT_He,'-',L,dT_Hemax,'*');
% legend ('dT-He','dT-Hemax',2);
% grid on;
% axis auto
% ylabel('dT_He [C]','FontSize',12);
% xlabel('Length [m]','FontSize',12);
% title('\it{dT_He vs. z}','FontSize',16);
% figure

T_UO2 = T_cladinside + dT_He % [C] Temperature on surface of uranium pin
T_UO2mean = 197; % Average temperature on surface of fuel pellet, from Safety
report
T_UO2max = 366; % Maximum temperature on surface of fuel pellet, from Safety
report

% plot(L,T_UO2,'-',L,T_UO2max,'*');
% legend ('T-UO2','T-UO2max',2);
% grid on;
% axis normal
% ylabel('T_UO2 [C]','FontSize',12);
% xlabel('Length [m]','FontSize',12);
% title('\it{T_UO2 vs. z}','FontSize',16);
% figure

k_UO2 = 2; % [W/m*K] Average conduction number for uraniumdioxide-pellet
T_c = T_UO2 + ((Q*Pf).*cos(z_vector))/(4*pi*N*n*z_scalar*k_UO2) % [degrees C]
Temperature at centre of fuel pellet
T_cmean = 622; % [C] Average centre temperature fuel pellet, from Safety
report
T_cmax = 1228 % [C] Maximum centre temperature of fuel pellet, from Safety
report

% plot(L,T_c,'-',L,T_cmax,'*');
% legend ('T-c','T-cmax',2);
% grid on;
% axis auto
% ylabel('T_c [C]','FontSize',12);
% xlabel('Length [m]','FontSize',12);
% title('\it{T_c vs. z}','FontSize',16);
% figure

% Tabulating the Nusselt number, the T_clad, the T_cladinside, the dT_He,
% the T_UO2 and the T_c for each Nusselt correlation

Table1(s,1)=max(Nu(s));
```

```
Table1(s,2)=max(T_clad);
Table1(s,3)=max(T_cladinside);
Table1(s,4)=max(dT_He);
Table1(s,5)=max(T_UO2);
Table1(s,6)=max(T_c);
xlswrite('temperatures2MW.xls',Table1)

figure('name','Temperatures for fuel element')

% Subplotting the temperatures for each Nusselt correlation

subplot(3,2,1), plot(T_clad)
grid off;
axis tight
set(gca,'xtick',7:12:200,'xTickLabel',{'5','','15','','25','','35','',...
'45','','55','','65','','75','','85'})
ylabel('T-clad [deg. C]','FontSize',12);
xlabel('Length [cm]','FontSize',12);
title('\it{Tclad vs. z}','FontSize',16);

subplot(3,2,2), plot(T_cladinside)
grid off;
axis tight
set(gca,'xtick',7:12:200,'xTickLabel',{'5','','15','','25','','35','',...
'45','','55','','65','','75','','85'})
ylabel('T-cladinside [deg. C]','FontSize',12);
xlabel('Length [cm]','FontSize',12);
title('\it{Tcladinside vs. z}','FontSize',16);

subplot(3,2,3), plot(dT_He)
grid off;
axis tight
set(gca,'xtick',7:12:200,'xTickLabel',{'5','','15','','25','','35','',...
'45','','55','','65','','75','','85'})
ylabel('dT-He [deg. C]','FontSize',12);
xlabel('Length [cm]','FontSize',12);
title('\it{dT-He vs. z}','FontSize',16);

subplot(3,2,4), plot(T_UO2)
grid off;
axis tight
set(gca,'xtick',7:12:200,'xTickLabel',{'5','','15','','25','','35','',...
'45','','55','','65','','75','','85'})
ylabel('T-UO2 [deg. C]','FontSize',12);
xlabel('Length [cm]','FontSize',12);
title('\it{T-UO2 vs. z}','FontSize',16);

subplot(3,2,5), plot(T_c)
grid off;
axis tight
set(gca,'xtick',7:12:200,'xTickLabel',{'5','','15','','25','','35','',...
'45','','55','','65','','75','','85'})
ylabel('T-c [deg. C]','FontSize',12);
xlabel('Length [cm]','FontSize',12);
title('\it{Tc vs. z}','FontSize',16);
```

```
% subplot(3,2,6), plot(Nu(s),'*')
% set(gca,'xtick',[])
% ylabel('Dimensionless','FontSize',12);
% title(['Nusselt value = ',num2str(Nu(s),'%.0f')],'FontSize',16);


h1 = subplot(321); % For the plotting of the Dittus-Boelter..
h2 = subplot(322); % ..to control the axis
h3 = subplot(323);
h4 = subplot(324);
h5 = subplot(325);
axis([h1 h2],[0 205 85 120]);
axis([h3],[0 205 130 270]);
axis([h4],[0 205 220 390]);
axis([h5],[0 205 600 1300])

ha = axes('Position',[0 0 1 1],'Xlim',[0 1],'Ylim',[0 1]...
,'Box','off','Visible','off','Units','normalized', 'clipping' , 'off');
% title(['Nusselt value = ',num2str(Nu(s),'%.0f')],'FontSize',16);
text(0.5, 1,['Temperature distributions for Nusselt value
',num2str(Nu(s),'%.0f')]...
,'HorizontalAlignment','center','VerticalAlignment', 'top', 'FontSize',18)


s = s+1; % Adding 1 to s for the for loop
end

'end' %#ok<NOPTS>
```

A2 Extrapolation to 5 MW

```
% ~~~~~~~~~~~~~~~~~~~~~~~~~~~~~~~~~~~~~~~~~~~~~~~~~~~~~~~~~~~~~~~~~~~~~~~~~~~~
%    Extrapolating the model of the 2 MW to 5 MW
%    By Erik Henriksen
% ~~~~~~~~~~~~~~~~~~~~~~~~~~~~~~~~~~~~~~~~~~~~~~~~~~~~~~~~~~~~~~~~~~~~~~~~~~~~

%    Assumptions taken
% 1. Continuous velocity distribution within shroud
% 2. The heavy water is always at its liquid phase
% 3. The shroud surfaces are smooth
% 4. A fully developed flow
% 5. Heat flux over element length follows a cosine distribution, implying a
cosine neutron flux distribution (NSI p. 315)
% 6. No heat transport in axial direction, fuel pin/diameter >10 neglect the
axial heat transfer within the fuel relative to the radial (NSI p.316)
% 7. Average thermal conductivities
% 8. Inlet water temperature t_in = 50 degrees Celsius
% 9. Outlet water temperature t_out = 56 degrees Celsius
% 10. All control rods out of the core, and a hot spot factor of 2.04
% 11. The fuel is unirradiated

clear all

N = 19;           % Number of fuel elements
n = 11;           % Number of fuel pins per element
d_f = 12.8*10^-3; % [m] Diameter of fuel pellet
D_o = 0.015;      % [m] outer diameter of pin
D_i = 0.013;      % [m] inner diameter of pin cladding
d_o = 0.087;      % [m] outer diameter of fuel element
d_i = 0.041;      % [m] inner diameter of fuel element
z_v = (-pi*0.325):0.01:(pi*0.325);   % [m] Active length of fuel pin, vector
z_s = 0.9;         % [m] Active length of pin, scalar

Q = 5*10^6; % [W] Power level of reactor
G = 235/3600; % [m^3/s] Volumetric flow rate of heavy water
T_in = 50; % Inlet temperature

q_av = (Q.*cos(z_v))/(N*n*pi*D_o*z_s); % [W/m^2] Average heat flux from a
fuel pin
Pf = 2.04; % Hot spot factor
q_max = Pf*q_av % [W/m^2] Maximum heat flux from a fuel pin
figure('name','Maximum heat flux')
plot(q_max)
axis tight
set(gca,'xtick',7:12:200,'xTickLabel',{'5', '10', '15',
'20','25','30','35',...
'40','45','50','55','60','65','70','75','80','85'})
ylabel('W/m^2 [C]','FontSize',12);
xlabel('Length [cm]','FontSize',12);
title('\it{Maximum heat flux}','FontSize',16);

% Guessing a temperature for the bulk of the water to find
```

```
% density and specific heat capacity for the T_out calculations

t=60; % The guess at the temperature

% 1-D interpolation

t_rho = 50:2:70;
c1 = [1095.650 1094.691 1093.733 1092.657 1091.703 1090.513...
    1089.443 1088.258 1087.075 1085.894 1084.716];
rho=interp1(t_rho,c1,t); % Interpolating for density of heavy water at t
degrees

t_mu = 50:10:70;
c2 = [651.2*10^-6 551.8*10^-6 475.7*10^-6];
mu=interp1(t_mu,c2,t); % Interpolating for dynamic viscosity of heavy water
at t degrees

t_cp = 50:5:70;
c3 = [4197.3 4196.4 4196.1 4196.5 4197.5];
c_p=interp1(t_cp,c3,t); % Interpolating for specific heat capacity of heavy
water at t degrees

t_k = 50:10:70;
c4 = [0.618 0.625 0.629];
k=interp1(t_k,c4,t); % Interpolating for thermal conductivity of heavy water
at t degrees

T_out = T_in + Q/(rho*G*c_p) % Here finding the outlet temperature of the
water

% After finding the outlet temperature, this is used to
% find new specs for the heavy water

rhonew = interp1(t_rho,c1,T_out);
munew = interp1(t_mu,c2,T_out);
c_pnew = interp1(t_cp,c3,T_out);
knew = interp1(t_k,c4,T_out);

Pr=(c_pnew*munew/knew); % Prandtl number from T_out
A =(pi/4)*((d_o)^2-(d_i)^2)-(n*pi/4*D_o^2) % [m^2] Area of fuel bundle, one
element
Wp = (pi*d_o+pi*d_i+n*pi*D_o); % [m] Wetted perimeter of flow
D_h = 4*A/Wp; % [m] Hydraulic diameter
v = (G/N)/A % [m/s] Velocity through one fuel element
Re = rho*v*D_h/mu; % Reynolds number

% Nusselt number and h calculations

Nu(1) = 0.023*(Re^0.8)*(Pr^0.4) % Dittus-Boelter
Nu(2) = 0.032*(Re^0.8)*(Pr^0.37)*(D_h/z_s)^0.054 % Nusselt number, from
Hernes - safety report
f = ((0.790*log(Re))-1.64)^-2; % Friction factor for smooth tubes from
Pethukov, Incropera p. 490
```

```
Nu(3) = ((f/8)*(Re-1000)*Pr)/(1+((12.7*(f/8)^0.5)*(Pr^0.66)-1)) % Gnielinski
p. 515 Incropera
CO = 1.07 + (900/Re) - (0.63/(1+10*Pr));
Nu(4) = ((f/8)*Re*Pr)/(CO + (12.7*(f/8)^0.5)*((Pr^0.66)-1)) % Petukhov Table
4.4 Kakac
B = (D_h/D_o);
C = 1+(0.912*(Re^-0.1)*(Pr^0.4)*(1-2.0043*exp(-B))); % C is equal to phi in
formula
Nu(5) = C*(0.023*(Re^0.8)*(Pr^0.4)) % Markozy p. 446 Nuclear Systems I,
Finite array "Nu is insensitive to the boundary conditions for Pr>0.7", Nu
are accurate to within 10 % when P/D > 1.12
A = 0.144*Re^0.25;
Nu(6) = (1+(A/(z_s/D_h)))*(C*(0.023*(Re^0.8)*(Pr^0.4))) % Overall heat
transfer coefficient, p.448 NSI, tubes with bell mouth. For L/D_h >
0.693Re^0.25
h = Nu.*k/D_h % [W/m^2*K] heat transfer coefficient

TNu = [Nu(1)' Nu(2)' Nu(3)' Nu(4)' Nu(5)' Nu(6)'];
xlswrite('Nusselt values five',TNu) % Tabulating the Nusselt numbers

Th = [h(1)' h(2)' h(3)' h(4)' h(5)' h(6)'];
xlswrite('Heat transfer coefficient five',Th) % Tabulating the heat transfer
coefficients

% Iterating for the six different correlations

s=1;
for s=1:6
    r = [h(1) h(2) h(3) h(4) h(5) h(6)];

T_clad = (q_max./r(s))+T_out % Finding the temperature of the cladding

% plot(L,T_clad)
% grid on;
% axis normal
% legend ('T-clad',5);
% ylabel('Tclad [C]','FontSize',12);
% xlabel('Length [m]','FontSize',12);
% title('\it{Tclad vs. z}','FontSize',16);
% figure

k_al = 221; % [W/m*K] At 100 degrees Celsius, conductivity coefficient, from
Hernes. Could possibly be higher, due to maximum heat flux (k at 120
degrees?)
% k_zr = 20.42; % [W/m*K] Zirconium thermal conductivity

% Temperature inside of the cladding
T_cladinside = T_clad + (log(D_o/D_i)*Q*Pf.*cos(z_v))/(z_s*N*n*2*pi*k_al) %
[C] Resistance equation, solved for temperature. Page 151 Yunus

% plot(L,T_cladinside)
% legend ('T-cladinside',2);
% grid on;
% axis auto
% ylabel('Tcladinside [C]','FontSize',12);
```

```
% xlabel('Length [m]','FontSize',12);
% title('\it{Tcladinside vs. z}','FontSize',16);
% figure

h_He = 2000; % [W/m^2*K] Heat transfer coefficient of He-layer, from Hernes
d_m = 0.01295; % [m] Mean diameter of He-layer
dT_He = ((Q*Pf).*cos(z_v))/(z_s*N*n*pi*d_m*h_He) % [C] Temperature rise
through He-layer, from Hernes

% plot(L,dT_He)
% legend ('dT-He',2);
% grid on;
% axis auto
% ylabel('dT-He [C]','FontSize',12);
% xlabel('Length [m]','FontSize',12);
% title('\it{dT-He vs. z}','FontSize',16);
% figure

T_UO2 = T_cladinside + dT_He % [C] Temperature on surface of uranium pin

% plot(L,T_UO2)
% legend ('T-UO2',2);
% grid on;
% axis normal
% ylabel('T-UO2 [C]','FontSize',12);
% xlabel('Length [m]','FontSize',12);
% title('\it{T-UO2 vs. z}','FontSize',16);
% figure

% Temperature at centre of fuel pellet
k_UO2 = 2; % [W/m*K] Average conduction number for uraniumdioxide-pellet
T_c = T_UO2 + (((Q*Pf).*cos(z_v))/(4*pi*N*n*z_s*k_UO2)) % [degrees C]
Temperature centre(Rafael)

% plot(L,T_c)
% legend ('T-c',2);
% grid on;
% axis auto
% ylabel('T-c [C]','FontSize',12);
% xlabel('Length [m]','FontSize',12);
% title('\it{T-c vs. z}','FontSize',16);
% figure

% Tabulating the Nusselt number, the T_clad, the T_cladinside, the dT_He,
% the T_UO2 and the T_c for each Nusselt correlation

Table2(s,1)=Nu(s);
Table2(s,2)=max(T_clad);
Table2(s,3)=max(T_cladinside);
Table2(s,4)=max(dT_He);
Table2(s,5)=max(T_UO2);
Table2(s,6)=max(T_c);
xlswrite('temperatures5MW.xls',Table2)
Table3=max((q_max/10^6));
xlswrite('fluxmax.xls',Table3)
```

```
figure('name','Temperatures for fuel element')

% Subplotting the temperatures for each Nusselt correlation

subplot(3,2,1), plot(T_clad)
grid off;
axis([0 210 80 120])
set(gca,'xtick',7:12:200,'xTickLabel',{'5', '10', '15',
'20','25','30','35',...
'40','45','50','55','60','65','70','75','80','85'})
ylabel('T-clad [deg. C]','FontSize',12);
xlabel('Length [cm]','FontSize',12);
title('\it{T-clad vs. z}','FontSize',16);

subplot(3,2,2), plot(T_cladinside)
grid off;
axis tight
set(gca,'xtick',7:12:200,'xTickLabel',{'5', '10', '15',
'20','25','30','35',...
'40','45','50','55','60','65','70','75','80','85'})
ylabel('T-cladinside [deg. C]','FontSize',12);
xlabel('Length [cm]','FontSize',12);
title('\it{T-cladinside vs. z}','FontSize',16);

subplot(3,2,3), plot(dT_He)
grid off;
axis tight
set(gca,'xtick',7:12:200,'xTickLabel',{'5', '10', '15',
'20','25','30','35',...
'40','45','50','55','60','65','70','75','80','85'})
ylabel('dT-He [deg. C]','FontSize',12);
xlabel('Length [cm]','FontSize',12);
title('\it{dT-He vs. z}','FontSize',16);

subplot(3,2,4), plot(T_UO2)
grid off;
axis tight
set(gca,'xtick',7:12:200,'xTickLabel',{'5', '10', '15',
'20','25','30','35',...
'40','45','50','55','60','65','70','75','80','85'})
ylabel('T-UO2 [deg. C]','FontSize',12);
xlabel('Length [cm]','FontSize',12);
title('\it{T-UO2 vs. z}','FontSize',16);

subplot(3,2,5), plot(T_c)
grid off;
axis tight
set(gca,'xtick',7:12:200,'xTickLabel',{'5', '10', '15',
'20','25','30','35',...
'40','45','50','55','60','65','70','75','80','85'})
ylabel('T-c [deg. C]','FontSize',12);
xlabel('Length [cm]','FontSize',12);
title('\it{Tc vs. z}','FontSize',16);
```

```
% subplot(3,2,6), plot(Nu(s),'*')
% set(gca,'xtick',[])
% ylabel('Dimensionless','FontSize',12);
% title(['Nusselt value = ',num2str(Nu(s),'%.0f')],'FontSize',16);

h1 = subplot(321); % For the plotting of the Markozy correlation..
h2 = subplot(322); % ..to control the axis
axis([h1 h2],[0 205 130 225])

ha = axes('Position',[0 0 1 1],'Xlim',[0 1],'Ylim',[0 1]...
,'Box','off','Visible','off','Units','normalized', 'clipping' , 'off');
% title(['Nusselt value = ',num2str(Nu(s),'%.0f')],'FontSize',16);
text(0.5, 1,['Temperature distributions for Nusselt value
',num2str(Nu(s),'%.0f')]...
,'HorizontalAlignment','center','VerticalAlignment', 'top', 'FontSize',18)

s = s+1; % Adding 1 to s for the for loop
end

'end' %#ok<NOPTS>
```

A3 Fuel capsule including a cross section of the shroud